MR Oct. 1942

NATIONAL ADVISORY COMMITTEE FOR AERONAUTICS

WARTIME REPORT

ORIGINALLY ISSUED

October 1942 as
Memorandum Report

AERODYNAMIC CHARACTERISTICS AND FLAP LOADS OF THE BRAKE-FLAP INSTALLATION ON THE 0.40-SCALE MODEL OF THE F4F-3 LEFT WING PANEL

By Paul E. Purser and Robert B. Liddell

Langley Memorial Aeronautical Laboratory
Langley Field, Va.

NACA

WASHINGTON

MEMORANDUM REPORT

for the

Bureau of Aeronautics, Navy Department

AERODYNAMIC CHARACTERISTICS AND FLAP LOADS OF THE BRAKE-FLAP INSTALLATION ON THE 0.40-SCALE MODEL OF THE F4F-3 LEFT WING PANEL

By Paul E. Purser and Robert B. Liddell

INTRODUCTION

At the request of the Bureau of Aeronautics, Navy Department, tests have been made in the LMAL 7- by 10-foot tunnel for determining the aerodynamic characteristics and the flap loads of a brake-flap installation on a 0.40-scale semispan model of the F4F-3 left wing panel. The data are presented in coefficient form and include lift, drag, and pitching-moment coefficients of the airfoil-flap combinations and the normal-force, chord-force, and hinge-moment coefficients of the upper (perforated split) flap and the lower (slotted) flap.

The flap loads and the airfoil characteristics agreed reasonably well with the values predicted from previous data when corrected for the flap spans, flap chords, aspect ratios, and perforations.

APPARATUS AND METHODS

Test Installation

A 0.40-scale semispan model of the F4F-3 left wing panel was suspended in the LMAL 7- by 10-foot tunnel (reference 1)

as shown schematically in figure 1 and in the photographs, figures 2(a) and 2(b). The root chord of the model was adjacent to one of the vertical walls of the tunnel, the vertical wall thereby serving as a reflection plane. The flow over a semispan in this set-up is essentially the same as it would be over a complete wing in a 7- by 20-foot tunnel. Although a very small clearance was maintained between the root chord of the model and the tunnel wall, no part of the model was fastened to or in contact with the tunnel wall. The model was suspended entirely from the balance frame, as shown in figure 1, in such a way that all the forces and moments acting on it might be determined. Provision was made for changing the angle of attack while the tunnel was in operation.

The flap loads were measured by three-component electrical strain-gage units located at each end of each flap as shown in the photograph (fig. 3). The two units on each flap were connected in series and the readings were taken from a control panel located outside the tunnel.

MODELS

The 0.40-scale semispan model of the F4F-3 wing was built to the plan form shown in figure 4 and represents the cross-hatched portion of the airplane shown in figure 5. The basic airfoil sections were of the NACA 230 series tapering in thickness from approximately 15$\frac{1}{2}$ percent at the root to 8$\frac{1}{4}$ percent

at the tip. The basic chord c_1 of the model was increased 0.3 inch to reduce the trailing-edge thickness and the last few stations were refaired to give a smooth contour. The ordinates of the extended and refaired sections are given in table I.

The lower (slotted) flap was that used in previous lateral-control investigations of the F4F-3 wing. The lower flap had a span of 52.3 inches and was approximately constant 20.7 percent chord. The flap and slot ordinates given in table II are for a full-span flap but only the inboard 52.3-inch portion of the flap span was used in the present investigation since the flap had been cut to that span for use in previous lateral-control investigations.

The upper (perforated split) flap was built in accordance with figure 6 and consisted of aluminum sheet screwed to steel ribs and spars. (See figs. 2 and 3.)

The upper and lower flaps were deflected along the path indicated by the data shown in table III. Both flaps were in the same location with respect to the tunnel wall as the location in which the proposed flaps would be with respect to the side of the airplane fuselage.

Test Conditions

All the tests were made at a dynamic pressure of 16.37 pounds per square foot which corresponds to a velocity of about 80 miles per hour and to a test Reynolds number of

2,050,000 based on the model wing mean aerodynamic chord of 33.66 inches. The effective Reynolds number of the tests was about 3,280,000 based on a turbulence factor of 1.6 for the LMAL 7- by 10-foot tunnel.

RESULTS AND DISCUSSION

Coefficients and Corrections

The coefficients used in the presentation of results are:

C_L airfoil lift coefficient, L/qS

C_D airfoil drag coefficient, D/qS

C_m airfoil pitching-moment coefficient about the 0.24 c_l line, M/qSc'

C_{N_f} flap normal-force coefficient, N_f/qS_f

C_{c_f} flap chord-force coefficient, C_f/qS_f

C_{h_f} flap hinge-moment coefficient, $H_f/qS_f\bar{c}_f$

c_l basic model wing chord at any spanwise location

c actual model wing chord at any spanwise location (basic model wing chord plus 0.3 in.)

c' model wing mean aerodynamic chord (33.66 in.)

S twice area of semispan wing model (41.60 sq ft)

S_f area of model flaps (upper, 2.159 sq ft; lower, 2.736 sq ft)

$\bar{c}_f$ root mean square chord of model flaps (upper, 0.591 ft; lower, 0.633 ft)

c_f chord of model flaps at any spanwise location

L twice lift on semispan model

D twice drag on semispan model

M twice pitching moment of semispan model

N_f normal force on model flap

C_f chord force on model flap

H_f hinge moment about model flap support axis (upper, $0.45\ c_{f_U}$; lower, $0.15\ c_{f_L}$) (See fig. 6.)

q dynamic pressure of air stream uncorrected for blocking, $\frac{1}{2}\rho V^2$

α angle of attack

δ_f flap deflection with respect to retracted position

The subscripts U and L refer to the upper and lower flaps, respectively.

Twice the actual lift, drag, pitching moment and area of the model were used in the reduction of the results of airfoil characteristics because the model represented half a complete wing. The drag coefficient and angle of attack have been corrected only in accordance with the theory of trailing-vortex images. No corrections have been applied to the flap loads and moments. No corrections have been applied to any of the results for blocking, for the effects of the support strut, or for the treatment of the inboard end of the wing; that is, the small gap between the wing and the wall, the leakage through the wall around the support tube, and the boundary layer at the wall.

Airfoil Characteristics

Effects of deflecting lower flap.- The effects of deflecting only the lower flap (upper flap retracted) are shown in figure 7. The increments of lift coefficient and pitching-moment coefficient at zero angle of attack agreed reasonably well with the section data of references 1 and 2 when account was taken of the flap chord, flap span, and aspect ratio. No attempt was made to predict the increments of drag coefficient from section data but the increment for a flap deflection of 40° at zero angle of attack agreed with the data of reference 3. Deflecting the lower flap 40° increased the maximum lift coefficient from 1.43 to 2.08.

Effects of deflecting upper flap.- The effects of deflecting only the upper flap (lower flap retracted) are shown in figure 8. At the low flap deflections the increments of lift and pitching-moment coefficient at zero angle of attack agreed reasonably well with the data of references 4 to 8 when corrected for flap span, flap location, aspect ratio, and perforations. At high flap deflections the increment of lift coefficient was smaller than predicted from the data of reference 4 and agreed reasonably well with the data of reference 5. The increment of pitching-moment coefficient was in agreement with the increment predicted from the data of both references 4 and 5. The increment

of drag coefficient resulting from deflecting the upper flap was lower than predicted from the data of reference 5 and 8.

Effects of deflecting upper and lower flaps together.- The effects of deflecting the upper and the lower flaps together are shown in figure 9. The increments of lift coefficient at zero angle of attack for the combination were about half the values obtained from the addition of increments from separate tests, and the increments of pitching-moment coefficient for the combination were from two-thirds to three-quarters of the values obtained by the addition of increments from separate tests. The difference in the lift coefficients and the difference in the pitching-moment coefficients are probably due to the blanketing effect of the upper flap on the flow over the upper surface of the lower (slotted) flap. The increments of drag coefficient for the combination were slightly lower at low flap deflections but slightly higher at high flap deflections than the values obtained by an addition of the increments from separate tests.

The effects of deflecting the lower flap with the upper flap at various constant settings are shown in figures 10 to 14 and exhibit the same general trend of characteristics noted in the preceding discussion.

Flap Loads

Effect of deflecting lower flap.- The effects of deflecting the lower flap on the flap loads are shown in figure 7. The increment of lower flap normal-force coefficient agreed with references 9 and 10 when the data were corrected for flap chord, flap span, and aspect ratio. The increment of flap hinge-moment coefficient was larger than would be indicated by the data of references 9 and 10, but this discrepancy could be due to the different slot shape changing the magnitude and location of the peak pressures on the flap. The increment of flap chord-force coefficient agreed with the previous data for flap deflections up to 20° and then became considerably smaller. This decrease in the increment of chord-force coefficient may have been due to the same reasons as stated above for the hinge-moment-coefficient discrepancy plus an induced drag factor for the finite span flap and skin-friction drag that was not measured in the pressure-distribution tests.

Effects of deflecting upper flap.- The effects of deflecting the upper flap on the flap loads are shown in figure 8. The increments of upper flap normal-force and hinge-moment coefficient agreed with the data of references 6, 9, and 11 when account was taken of flap span, flap location, aspect ratio, and perforations. No previous data were available for comparisons of chord-force coefficients.

Effects of upper flap on lower flap loads.- The effects of the upper flap on the lower flap loads may be determined from comparisons of the data given in figures 10 to 14. At zero angle of attack the lower flap normal-force coefficients for lower flap deflections above 10° showed a sharp decrease of about 20 percent with initial upper flap deflection and then a gradual increase until at $\delta_{f_U} = 77°$ the lower flap normal-force coefficients were only about 15 percent lower than the values at $\delta_{f_U} = 0°$. The same variation occurred to a lesser extent and in a more inconsistent manner for the lower flap chord-force and hinge-moment coefficients when the upper flap was deflected.

Effects of lower flap on upper flap loads.- The effects of the lower flap on the upper flap loads may be determined from figures 10 to 14. In general, the normal-force coefficient of the upper flap increased about 0.005 per degree of lower flap deflection. The upper flap chord-force and hinge-moment coefficients generally showed a small, but inconsistent, increase with lower flap deflection.

APPLICATION OF DATA

Aerodynamic Characteristics

Methods of application.- In order to simplify the application of the aerodynamic data on the brake-flap installation the data of figures 7 to 14 were replotted in figure 15 against upper and lower flap deflection in the form of contours

of lift, drag, and pitching-moment coefficients at zero angle of attack. From figure 15 it is possible to determine the wing aerodynamic characteristics at zero angle of attack for any ratio of upper and lower flap deflections or to determine the flap deflection ratio necessary to produce the desired wing aerodynamic characteristics.

Using the contours of figure 15 and the application methods presented in reference 12 it was possible to compute the time-history characteristics of the F4F-3 airplane equipped with brake flaps. The changes in thrust and in drag coefficient (due to angle-of-attack change) during deceleration were neglected in the computations.

Results of application.- The time-history characteristics of the airplane were computed for several conditions. With a constant deceleration of 1.0g the characteristics were computed for zero angle-of-attack change during deceleration and also for minimum wing pitching-moment-coefficient change (fig. 16). As can be seen from figure 16 the condition of zero angle-of-attack change and minimum wing pitching-moment-coefficient change cannot be satisfied simultaneously. The optimum flap-deflection ratio in a practical installation would probably lie somewhere between that of the two sets of curves in figure 16 since the pilot, in keeping his sights on the target, would move his controls to counteract changes in both angle of attack and pitching

moment. It is pointed out that the pitching-moment coefficients presented in this report are for the wing alone and that formulation of conclusions as to the effects of the brake flaps on the airplane stability and control characteristics should await the results of tests of the complete model.

There appears to be some question as to the magnitude of the deceleration which would be acceptable to fighter pilots and for this reason computations were made for several values of deceleration. The time-history characteristics of the airplane with the flap-deflection ratio for minimum wing pitching-moment-coefficient change were computed and are presented in figure 17 for the following cases: deceleration of 1.5g maximum, then decreasing; 1.0g constant; 1.0g maximum, then decreasing; and 0.75g constant. The estimated time required to decelerate from 400 to 300 miles per hour for the several cases were respectively: $4\frac{1}{4}$, $5\frac{1}{2}$, $6\frac{1}{2}$, and 7 seconds. It is worthy of note that if the lower deceleration of 0.75g is satisfactory the flap span may be reduced and thus reduce the likelihood of wake interference on the tail of the airplane.

CONCLUSIONS

The results of the tests and computations indicated that at sea level at 400 miles per hour the brake flap installation on the F4F-3 airplane would give the following

characteristics: decelerate to 300 miles per hour in between $4\frac{1}{4}$ and 7 seconds with maximum accelerations between $1\frac{1}{2}$ and $\frac{3}{4}g$, an angle-of-attack change of about 2°, and a wing pitching-moment-coefficient change of about -0.03. The effects of the flaps on the airplane stability and control characteristics should be determined from tests of the complete model.

Langley Memorial Aeronautical Laboratory,
National Advisory Committee for Aeronautics,
Langley Field, Va., October 15, 1942.

REFERENCES

1. Wenzinger, Carl J., and Harris, Thomas A.: Wind-Tunnel Investigation of an N.A.C.A. 23012 Airfoil with Various Arrangements of Slotted Flaps. Rep. No. 664, NACA, 1939.

2. Wenzinger, Carl J., and Harris, Thomas A.: Wind-Tunnel Investigation of an N.A.C.A. 23021 Airfoil with Various Arrangements of Slotted Flaps. Rep. No. 677, NACA, 1939.

3. House, Rufus O.: The Effects of Partial-Span Slotted Flaps on the Aerodynamic Characteristics of a Rectangular and a Tapered N.A.C.A. 23012 Wing. T.N. No. 719, NACA, 1939.

4. Wenzinger, Carl J., and Harris, Thomas A.: Wind-Tunnel Investigation of N.A.C.A. 23012, 23021, and 23030 Airfoils with Various Sizes of Split Flap. Rep. No. 668, NACA, 1939.

5. Weick, Fred E., and Harris, Thomas A.: The Aerodynamic Characteristics of a Model Wing Having a Split Flap Deflected Downward and Moved to the Rear. T.N. No. 422, NACA, 1932.

6. Wallace, Rudolf: Investigation of Full-Scale Split Trailing-Edge Wing Flaps with Various Chords and Hinge Locations. Rep. No. 539, NACA, 1935.

7. Wenzinger, Carl J.: The Effect of Partial-Span Split Flaps on the Aerodynamic Characteristics of a Clark Y Wing. T.N. No. 472, NACA, 1933.

8. Purser, Paul E., and Turner, Thomas R.: Wind-Tunnel Investigation of Perforated Split Flaps for Use as Dive Brakes on a Rectangular NACA 23012 Airfoil. NACA A.C.R., July 1941.

9. Harris, Thomas A., and Lowry, John G.: Pressure Distribution Over an NACA 23021 Airfoil with a Slotted and a Split Flap. Rep. No. 718, NACA, 1941.

10. Wenzinger, Carl J., and Delano, James B.: Pressure Distribution over an N.A.C.A. 23012 Airfoil with a Slotted and a Plain Flap. Rep. No. 633, NACA, 1938.

11. Wenzinger, Carl J., and Harris, Thomas A.: Pressure Distribution over a Rectangular Airfoil with a Partial-Span Split Flap. Rep. No. 571, NACA, 1936.

12. Purser, Paul E.: A Study of the Application of Data on Various Types of Flap to the Design of Fighter Brakes. NACA A.C.R., June 1942.

L-549

TABLE I

ORDINATES FOR AIRFOIL

[Spanwise stations in inches from root section. Chord stations and ordinates in percent of basic wing chord c_1]

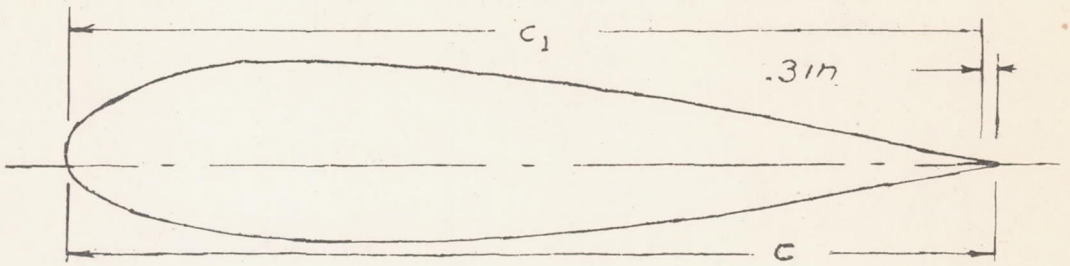

Model wing station 0		
Station	Upper surface	Lower surface
0	0	0
1.25	3.48	-1.60
2.5	4.61	-2.36
5	6.10	-3.21
7.5	7.14	-3.82
10	7.89	-4.33
15	8.80	-5.12
20	9.22	-5.71
25	9.40	-6.10
30	9.37	-6.28
40	8.90	-6.23
50	8.02	-5.78
60	6.85	-5.05
70	5.44	-4.10
80	3.87	-2.97
90	2.12	-1.67
95	1.16	-.94
100	.18	-.16
100.73	.03	-.03
L.E. radius: 2.65. Slope of radius through end of chord: 0.305		

Model wing station 88.8		
Station	Upper surface	Lower surface
0	0	0
1.25	1.89	-.84
2.5	2.65	-1.07
5	3.70	-1.26
7.5	4.45	-1.40
10	4.98	-1.52
15	5.54	-1.86
20	5.73	-2.22
25	5.77	-2.46
30	5.71	-2.62
40	5.36	-2.70
50	4.78	-2.56
60	4.06	-2.27
70	3.21	-1.87
80	2.26	-1.36
90	1.22	-.78
95	.70	-.46
100	.18	-.14
101.2	.05	-.05
L.E. radius: 0.70. Slope of radius through end of chord: 0.305		

L-549

TABLE II

ORDINATES FOR FLAP AND SLOT SHAPES

[Spanwise stations in inches from root section. Chord stations and ordinates in percent of basic wing chord c_1]

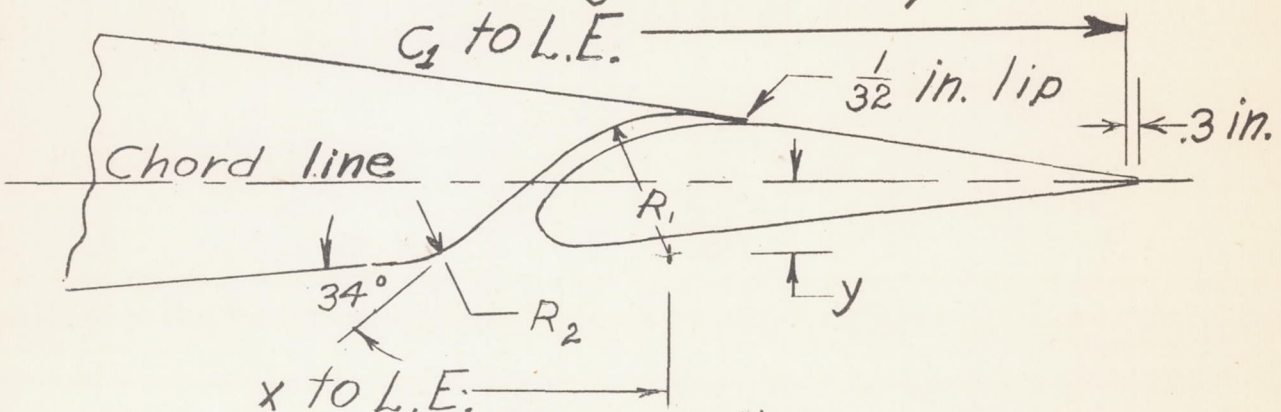

Flap stations

Model wing sta. 0			Model wing Sta. 88.8		
Sta.	Upper surface	Lower surface	Sta.	Upper surface	Lower surface
0	- 1.29	-1.29	0	-0.76	-0.76
.52	- .08	-2.30	.53	.01	-1.16
1.04	.48	-2.50	1.06	.36	-1.23
2.07	1.29	-2.60	2.12	.80	-1.22
4.15	2.17	-2.44	4.24	1.30	-1.10
6.22	2.53	-2.18	6.36	1.42	-.99
8.29	2.40	-1.91	8.48	1.35	-.87
12.44	1.65	-1.32	12.72	.93	-.62
16.58	.85	-.69	16.96	.51	-.32
20.72	.03	-.03	21.20	.05	-.05
L.E. radius: 1.19			L.E. radius: 0.32		

Slot Shape

	Station 0	Station 88.8
R_1	5.3	5.1
R_2	2	.2
x	85	83.3
y	2.5	3.3

NATIONAL ADVISORY
COMMITTEE FOR AERONAUTICS

L-549

TABLE III

Upper and lower flap locations. Brake flaps on 0.40-scale F4F-3 semispan wing model.

[Section 1 and 2 refer to the inboard and outboard spanwise positions, respectively]

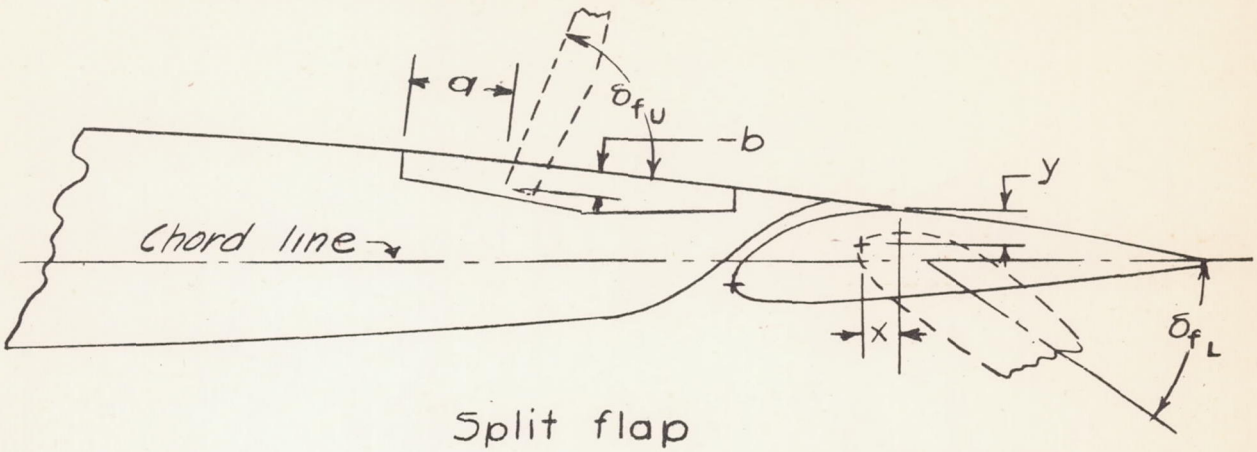

Split flap

Flap deflection	Section 1		Section 2	
	a, in.	b, in.	a, in.	b, in.
0	0	0	0	0
14.5	.05	.06	.09	.09
24.7	.32	.16	.37	.18
44.2	1.17	.11	1.26	.18
63.9	2.05	- .37	2.15	- .26
77.0	2.58	- .87	2.67	- .72

Slotted flap

Flap deflection	Section 1		Section 2	
	x, in.	y, in.	x, in.	y, in.
0	3.06	1.51	2.36	1.02
5	2.03	1.51	2.03	1.19
10	1.85	1.55	1.85	1.23
20	1.40	1.52	1.40	1.20
30	.97	1.42	.97	1.00
40	.68	1.05	.68	.72

NATIONAL ADVISORY
COMMITTEE FOR AERONAUTICS

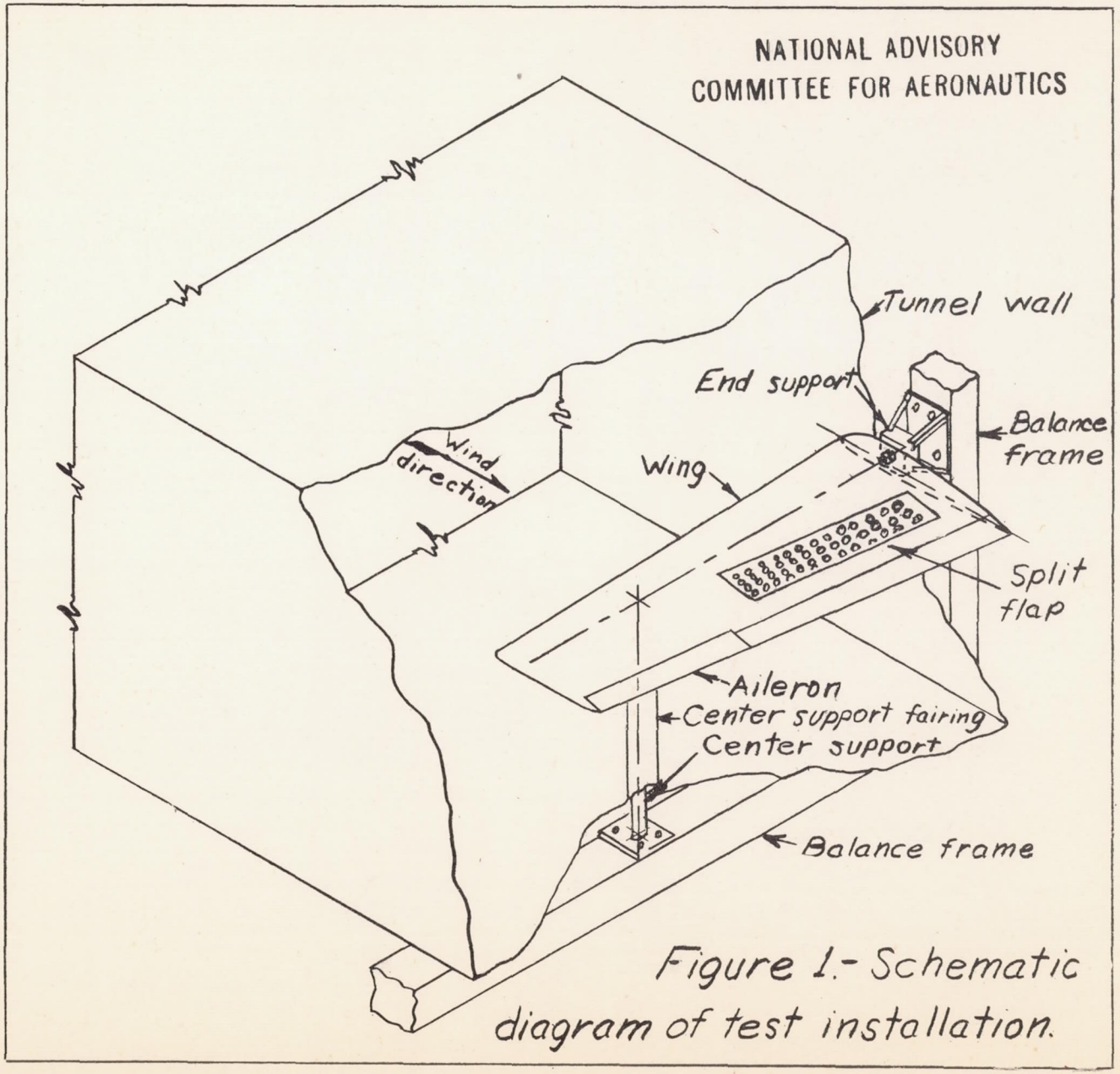

Figure 1.- Schematic diagram of test installation.

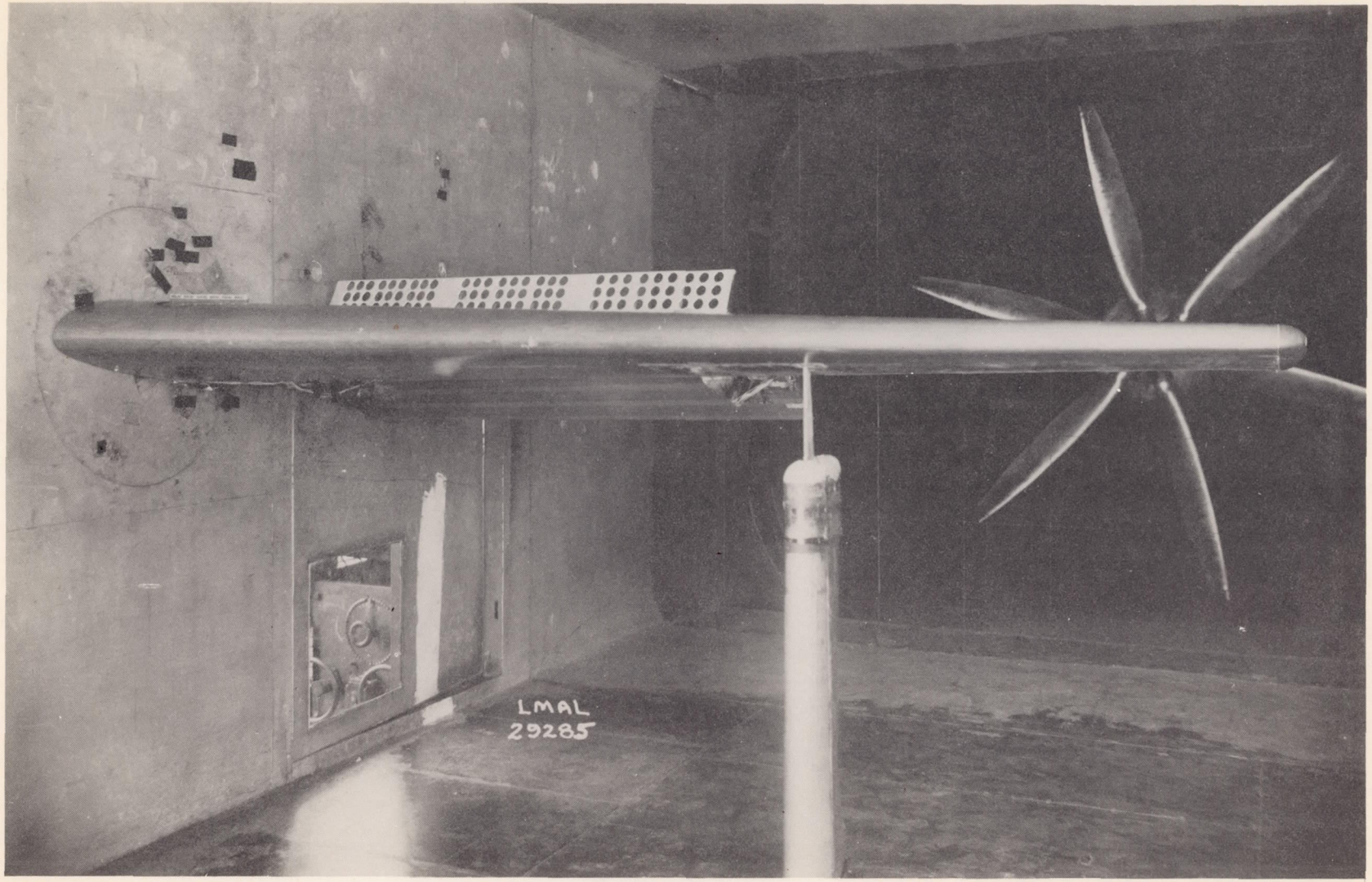

(a) Three-quarter front view.

Figure 2.- The 0.40-scale semispan model of the F4F-3 airplane wing mounted in the LMAL 7- by 10-foot tunnel.

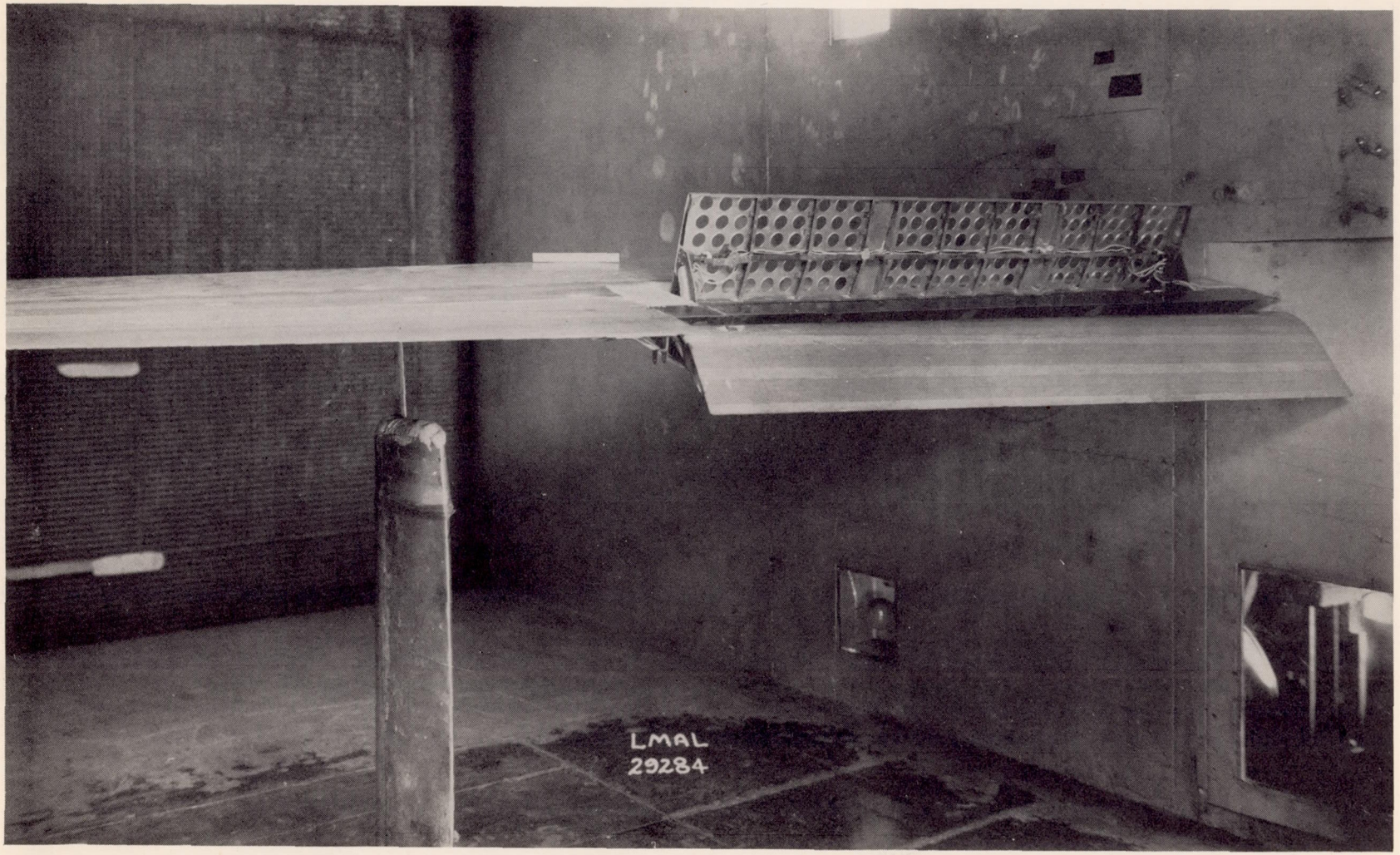

(b) Three-quarter rear view.

Figure 2.- The 0.40-scale semispan model of the F4F-3 airplane wing mounted in the LMAL 7- by 10-foot tunnel.

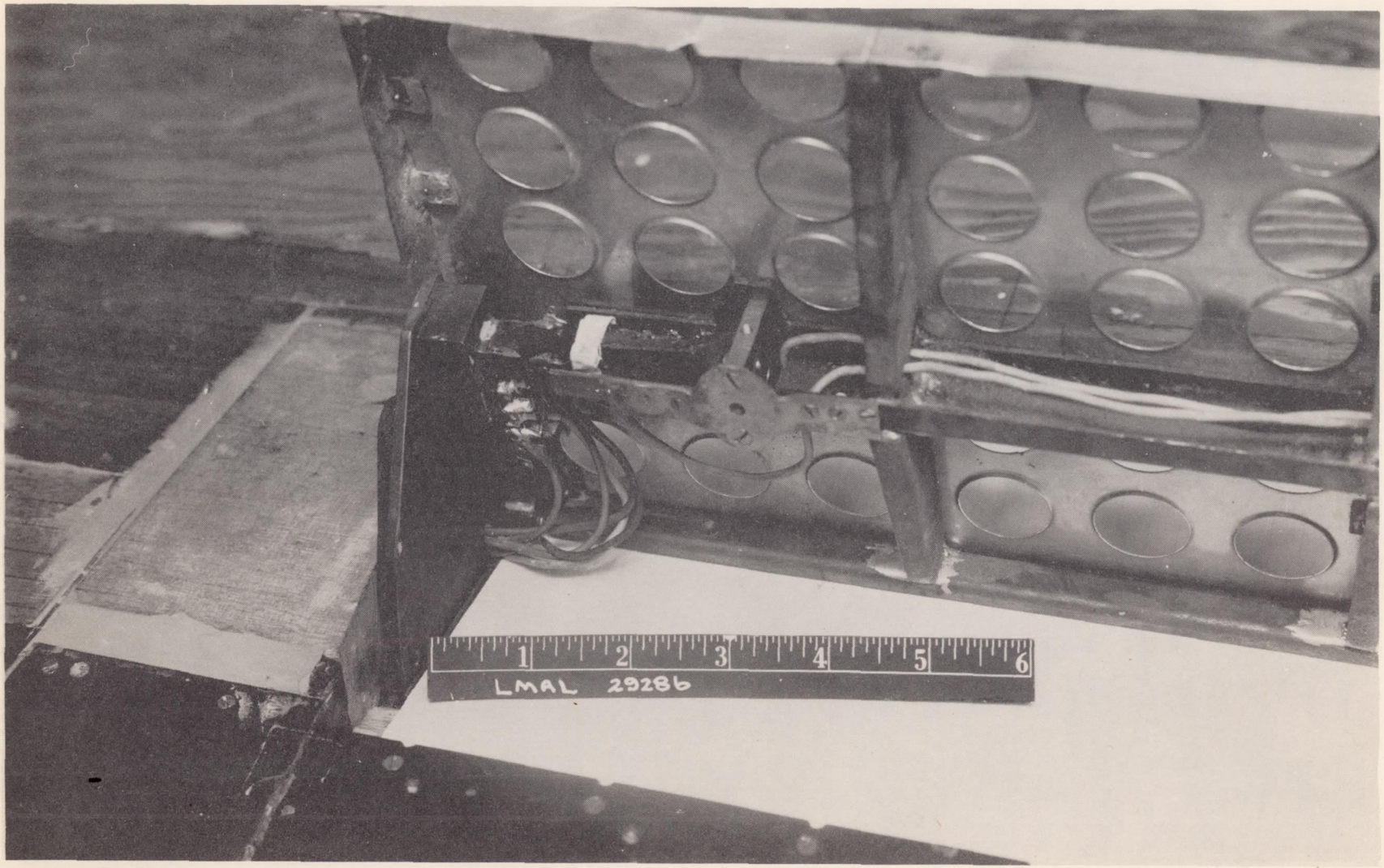

Figure 3.- Electrical strain-gage unit used for measuring flap loads on the brake-flap installation on the 0.40-scale semispan model of the F4F-3 airplane wing.

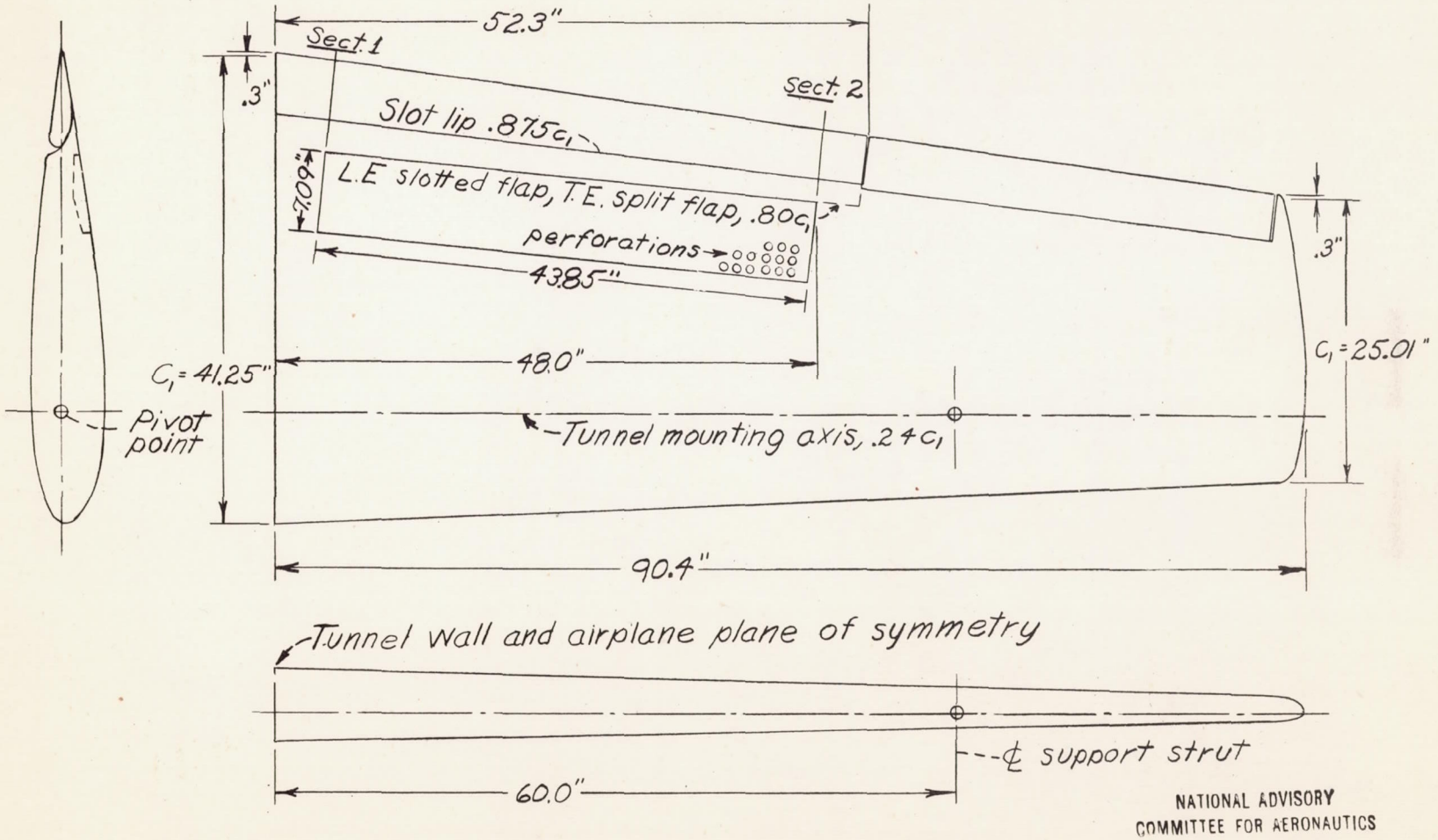

Figure 4 :- Semispan 0.40-scale model of F4F-3 left wing panel.

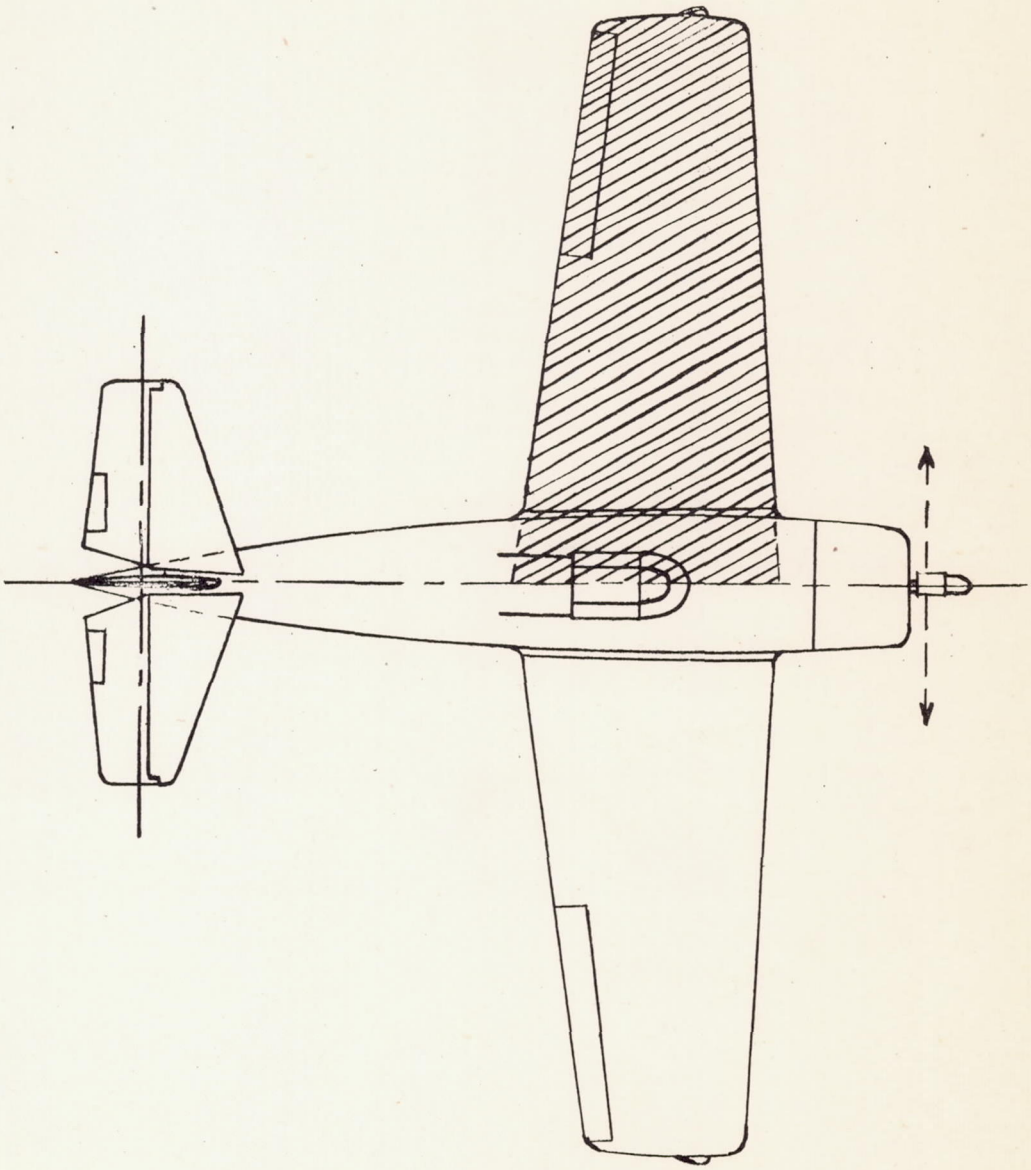

NATIONAL ADVISORY
COMMITTEE FOR AERONAUTICS

Figure 5.- Portion of airplane simulated by model.

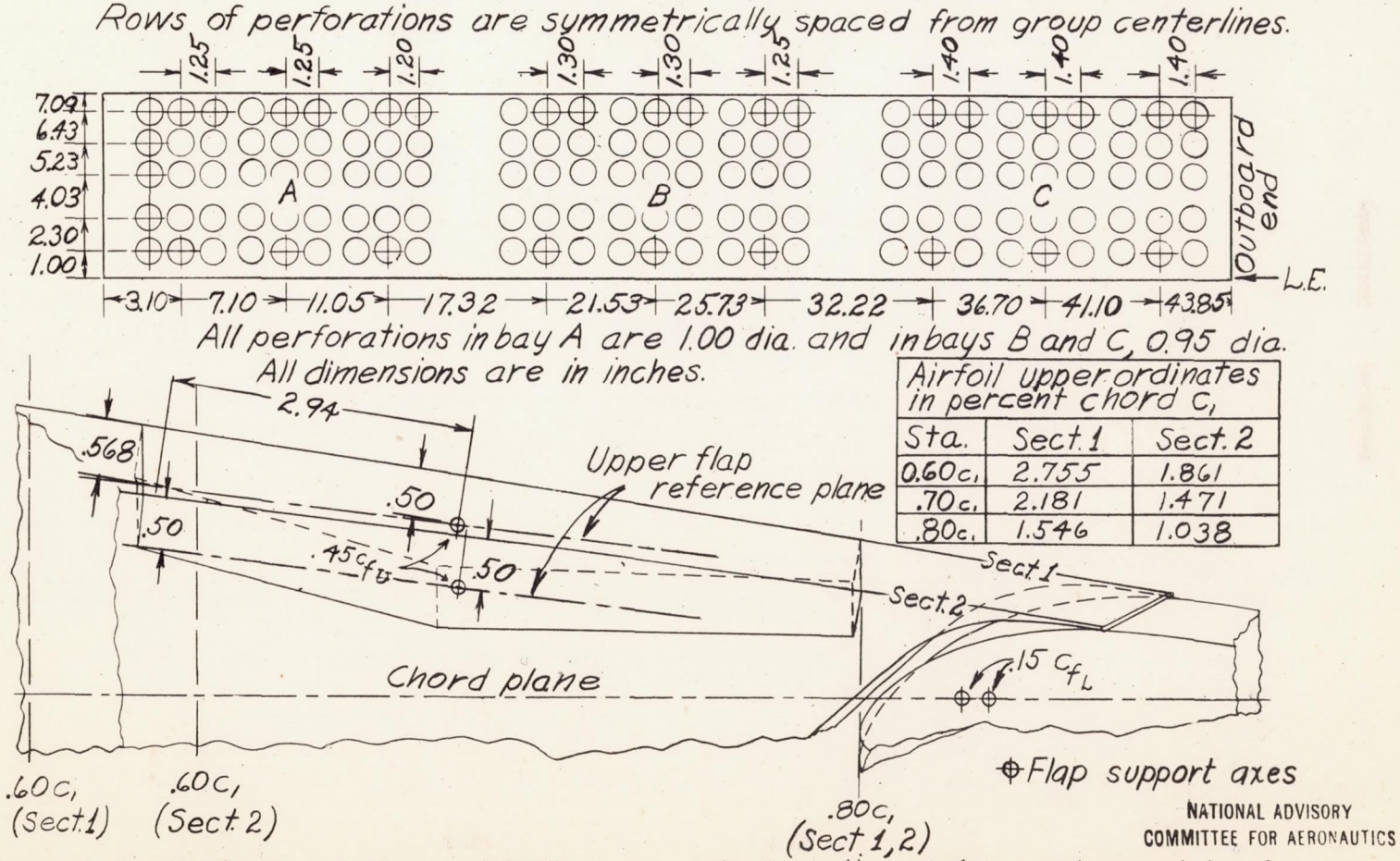

Airfoil upper ordinates in percent chord c_1

Sta.	Sect. 1	Sect. 2
0.60 c_1	2.755	1.861
.70 c_1	2.181	1.471
.80 c_1	1.546	1.038

NATIONAL ADVISORY COMMITTEE FOR AERONAUTICS

Figure 6.- Details of the split flap mounted on the 0.40-scale model of the F4F-3 wing panel.

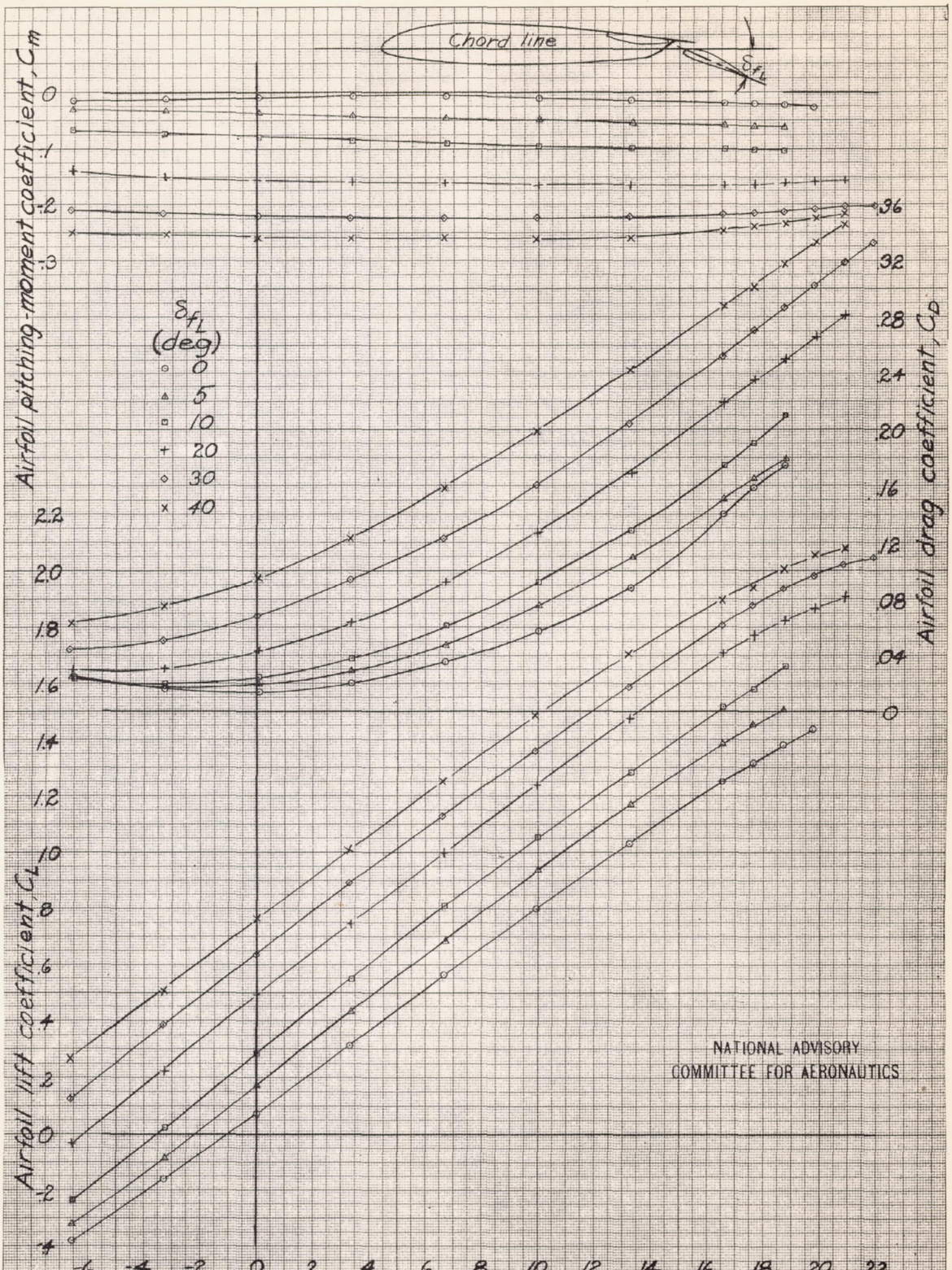

(a) Airfoil.

Figure 7.- Effect of lower flap deflection on the airfoil characteristics and flap loads of the brake-flap installation on the 0.40-scale model of the F4F-3 wing panel. Upper flap retracted.

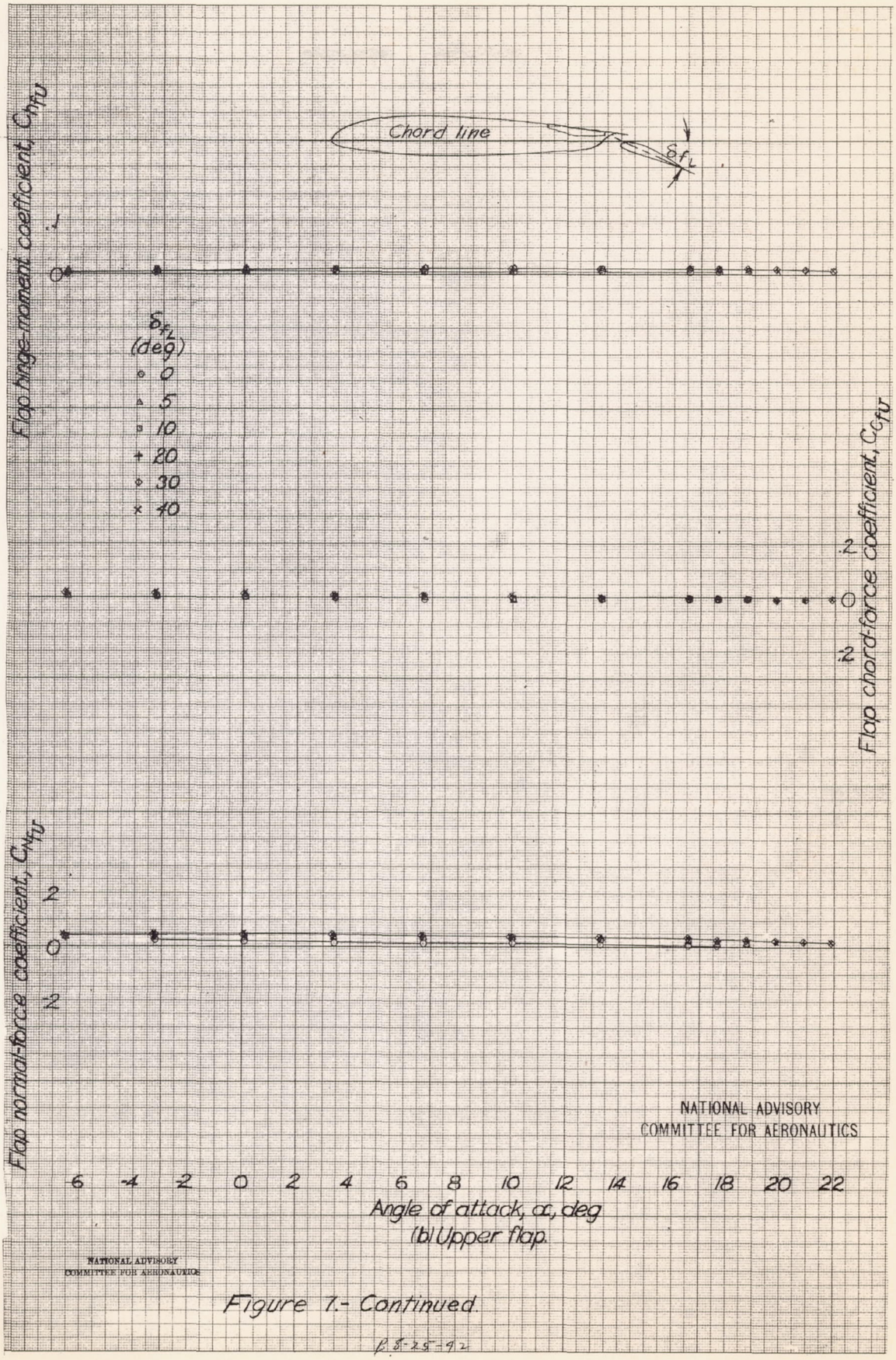

(b) Upper flap.

Figure 7.- Continued.

B.S-25-42

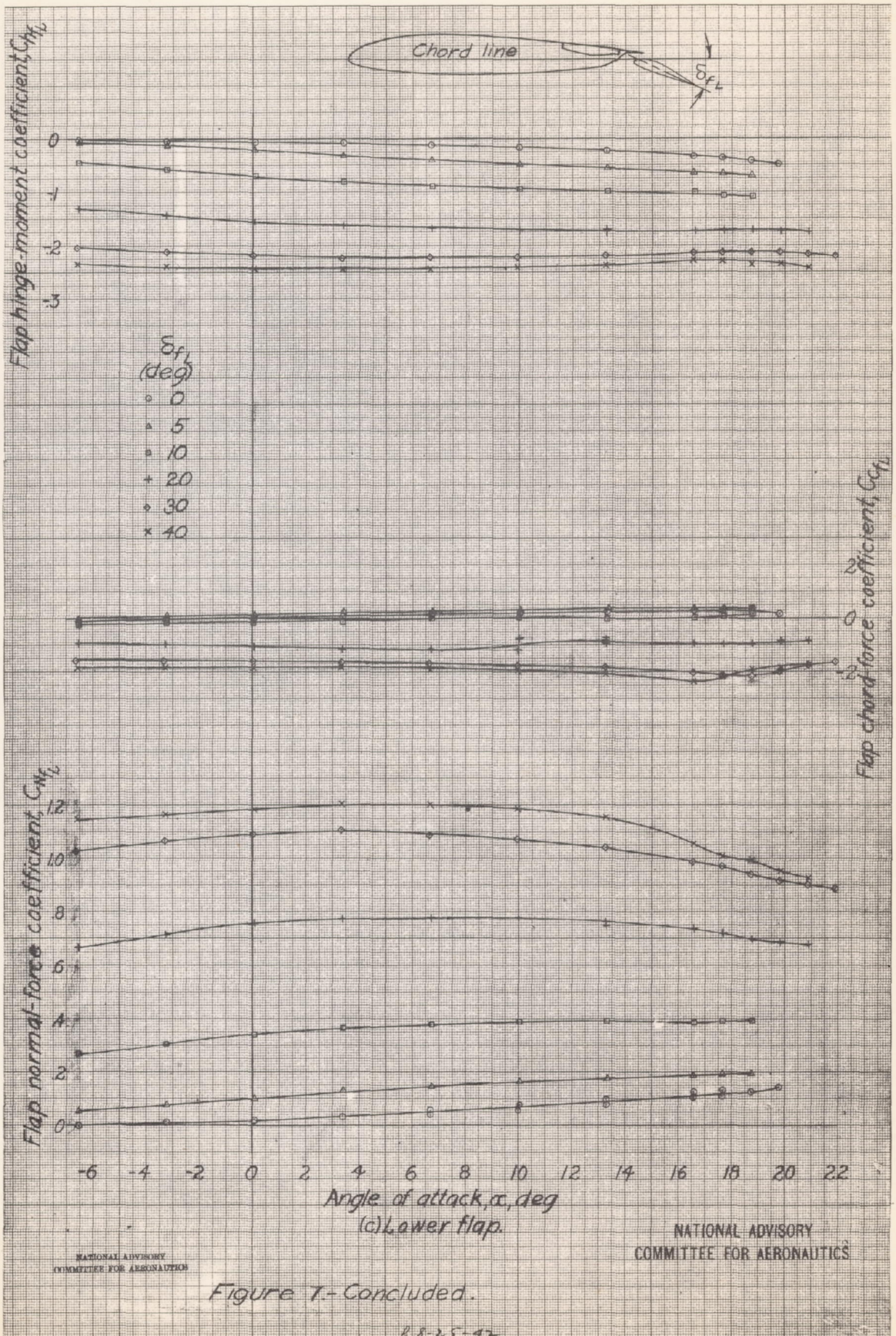

NATIONAL ADVISORY COMMITTEE FOR AERONAUTICS

Figure 7.- Concluded.

8-25-47

L-549.

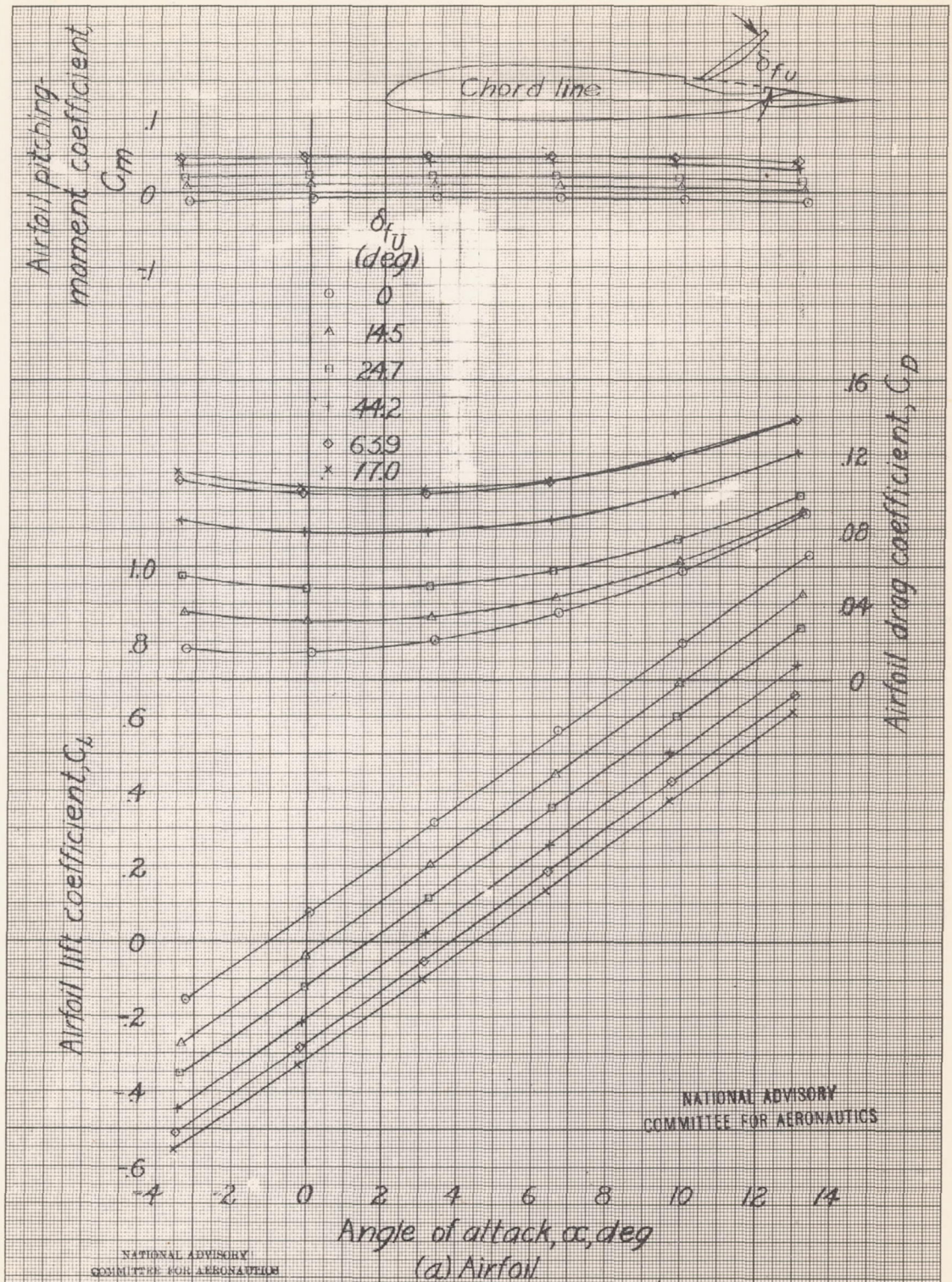

(a) Airfoil

Figure 8.- Effect of upper flap deflection on the airfoil characteristics and flap loads of the brake-flap installation on the 0.40-scale model of the F4F-3 wing panel. Lower flap retracted.

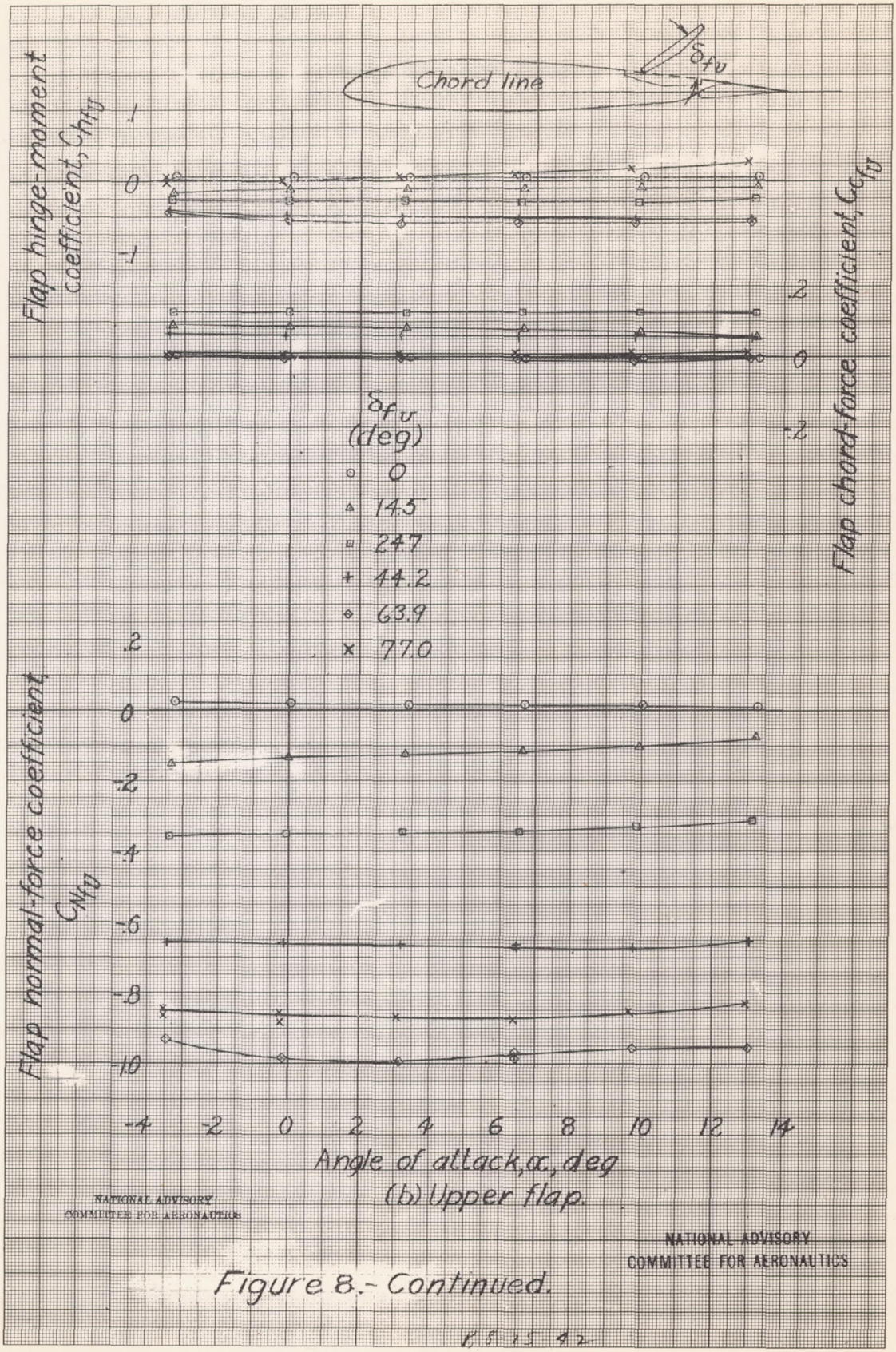

Figure 8.- Continued.

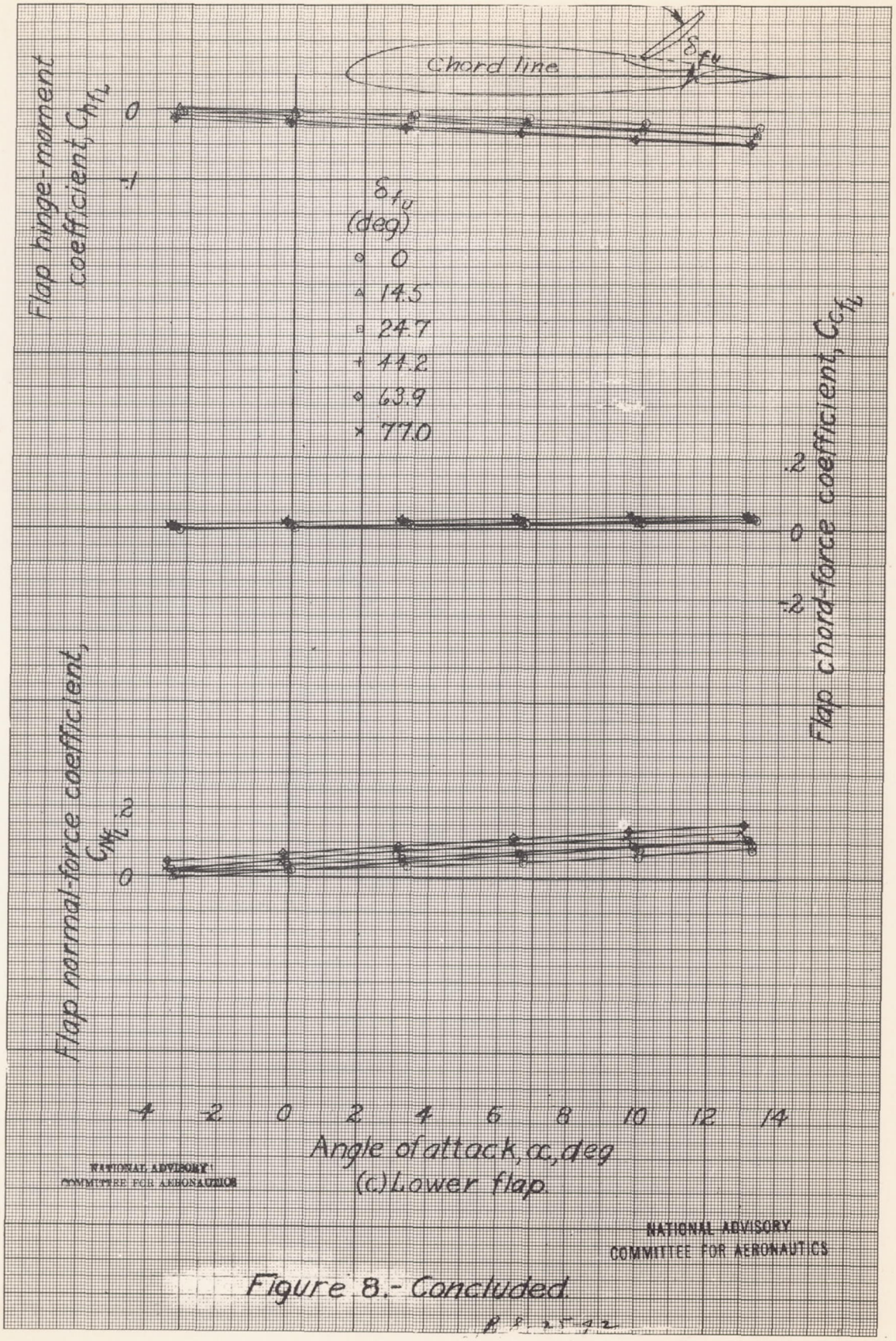

Figure 8.- Concluded.

L-549

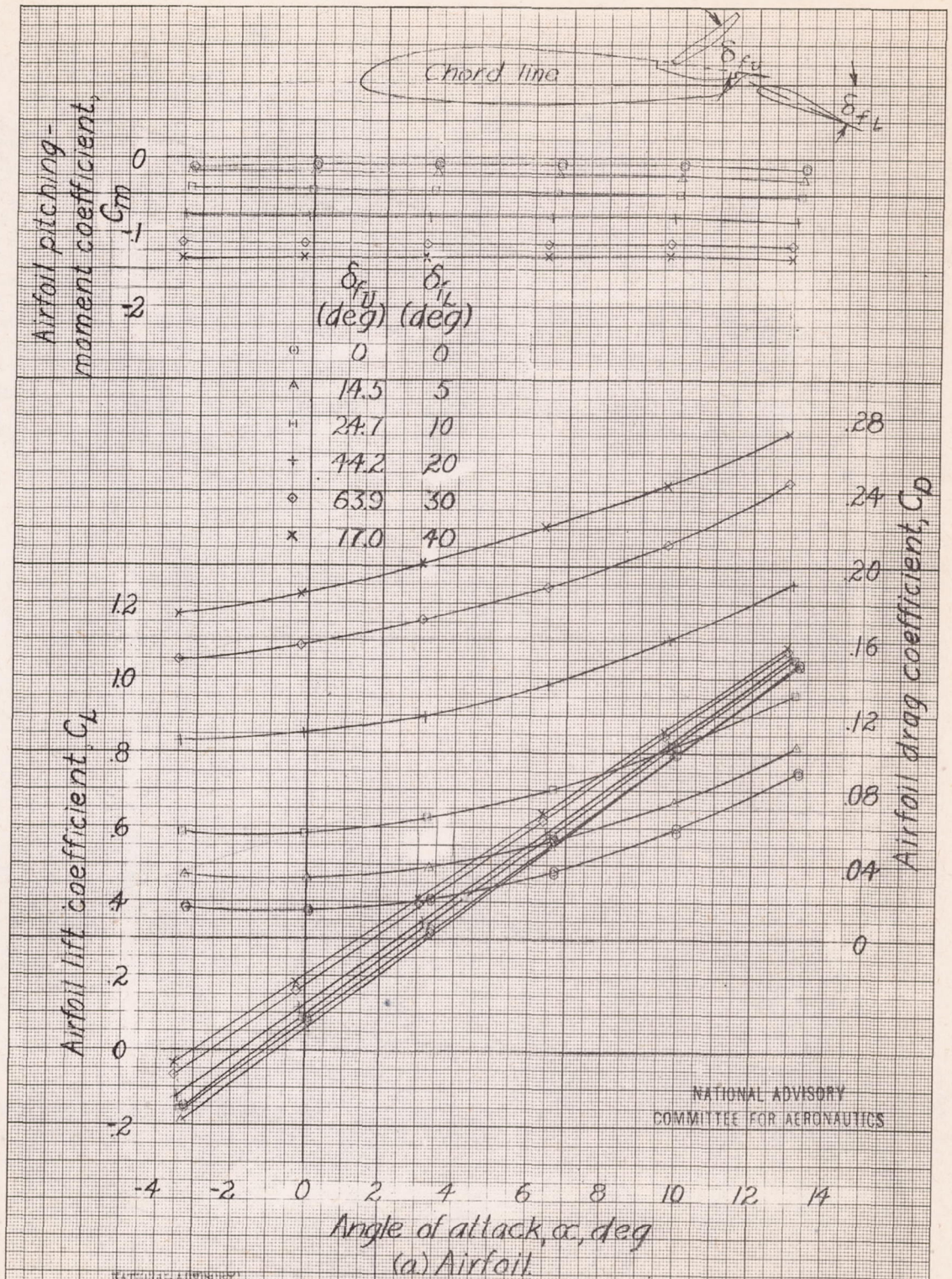

Figure 9.- Effect of upper and lower flap deflection on the airfoil characteristics and flap loads of the brake-flap installation on the 0.40-scale model of the YF-3 wing panel.

L-549

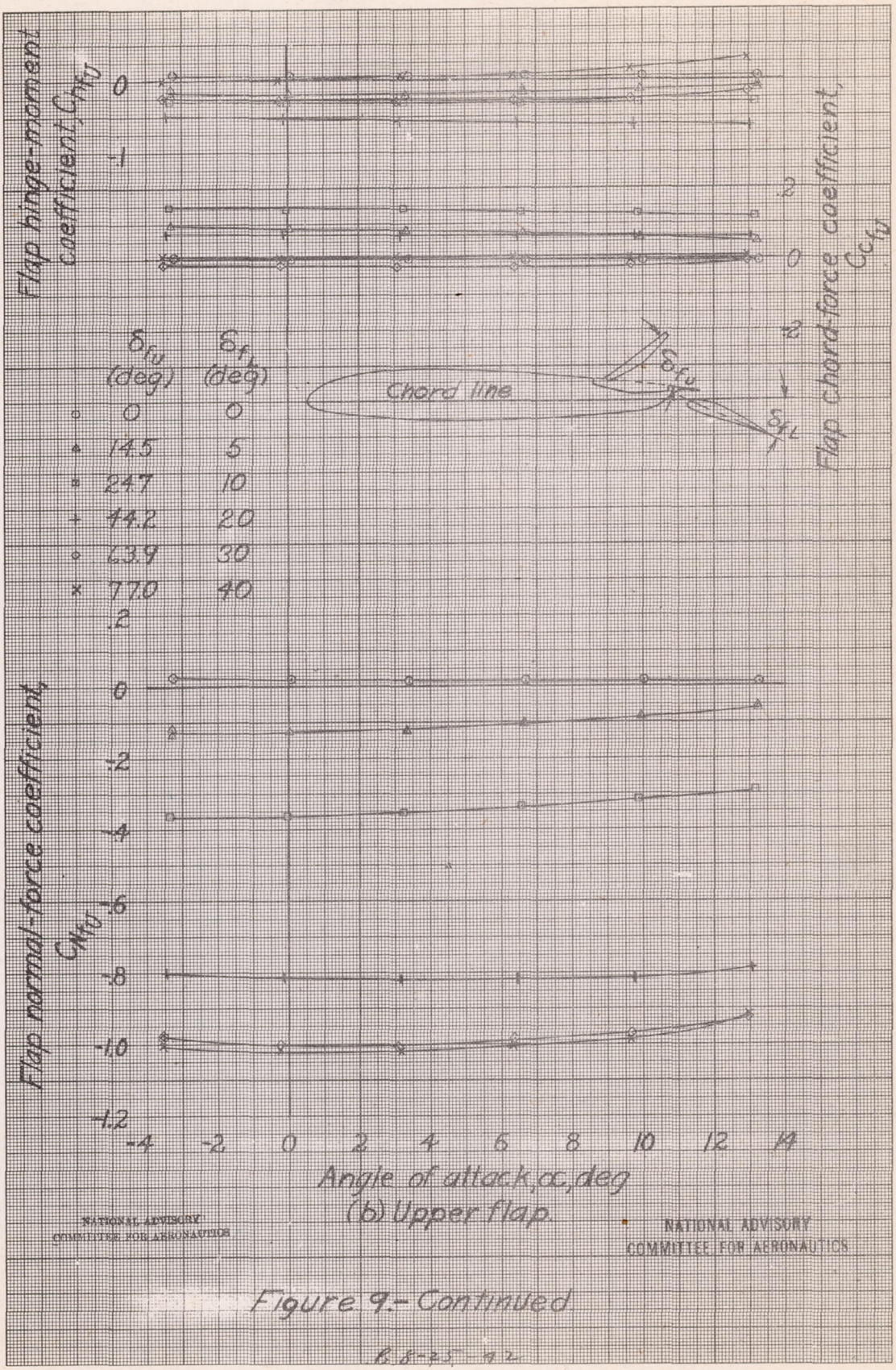

Figure 9.- Continued

L-549

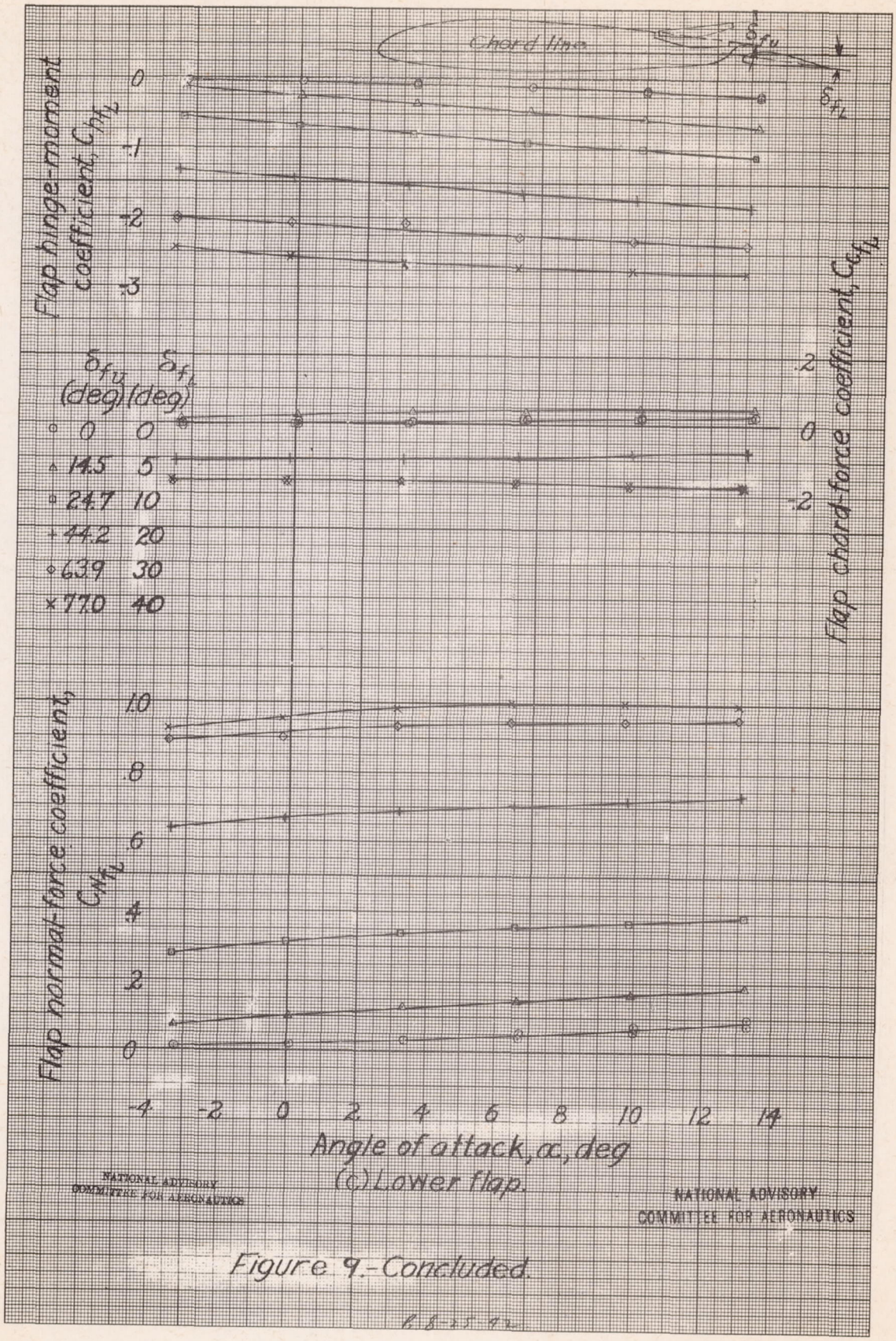

Figure 9.- Concluded.

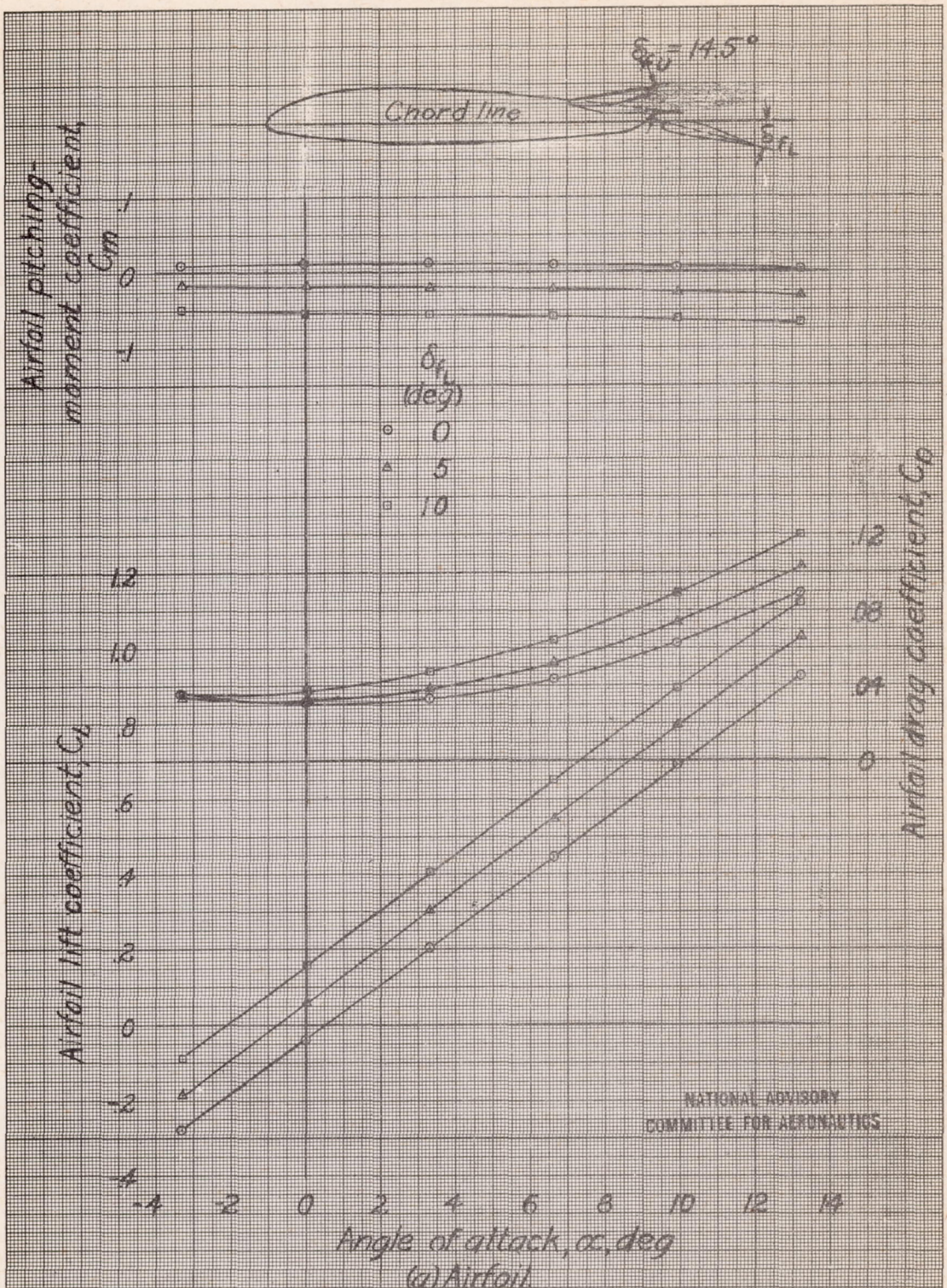

(a) Airfoil.

Figure 10.- Effect of lower flap deflection on the airfoil characteristics and flap loads of the brake-flap installation on the 0.40-scale model of the F4F-3 wing panel. δ_{f_o}, 14.5°.

L-549

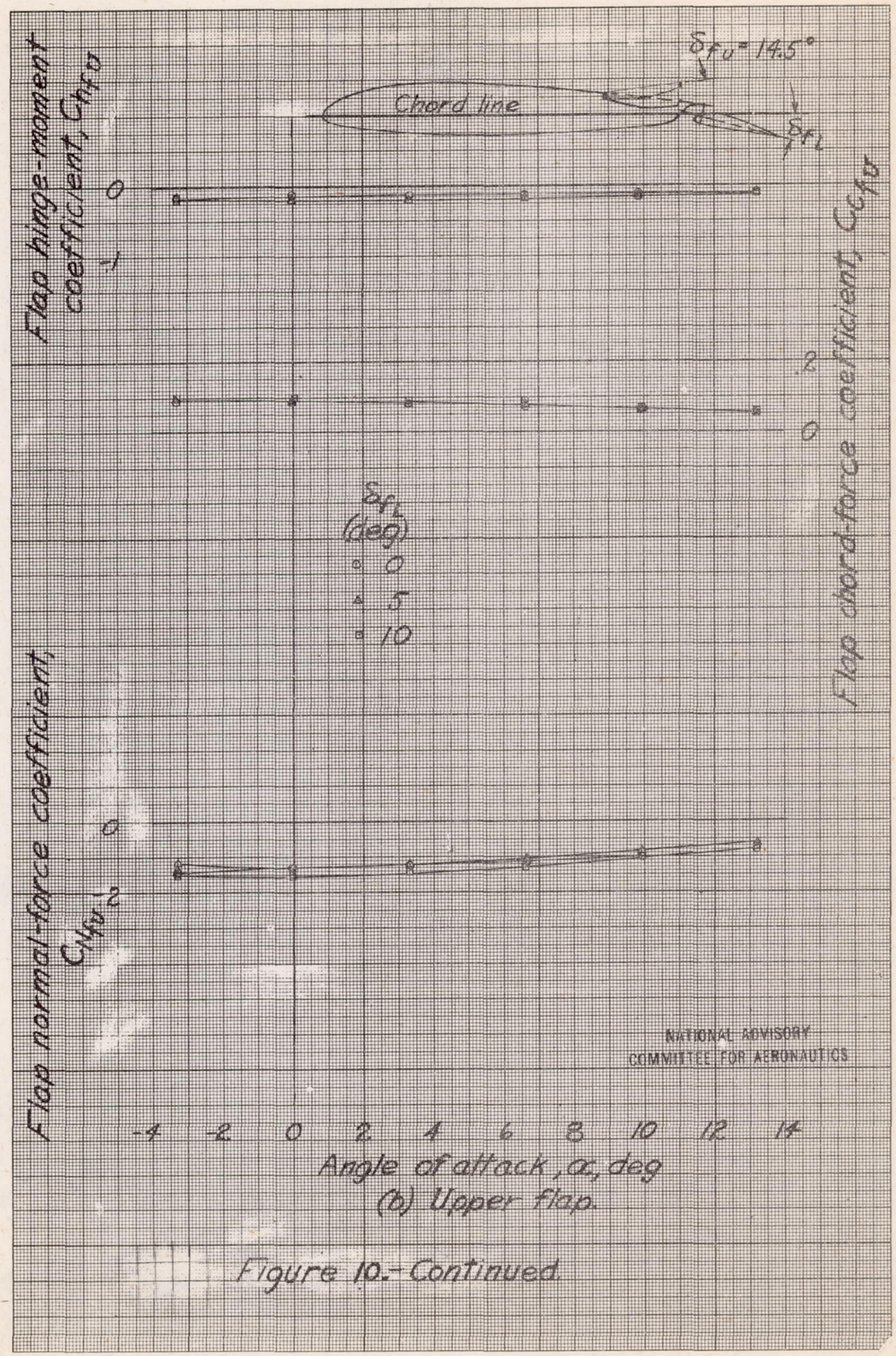

(b) Upper flap.

Figure 10.- Continued.

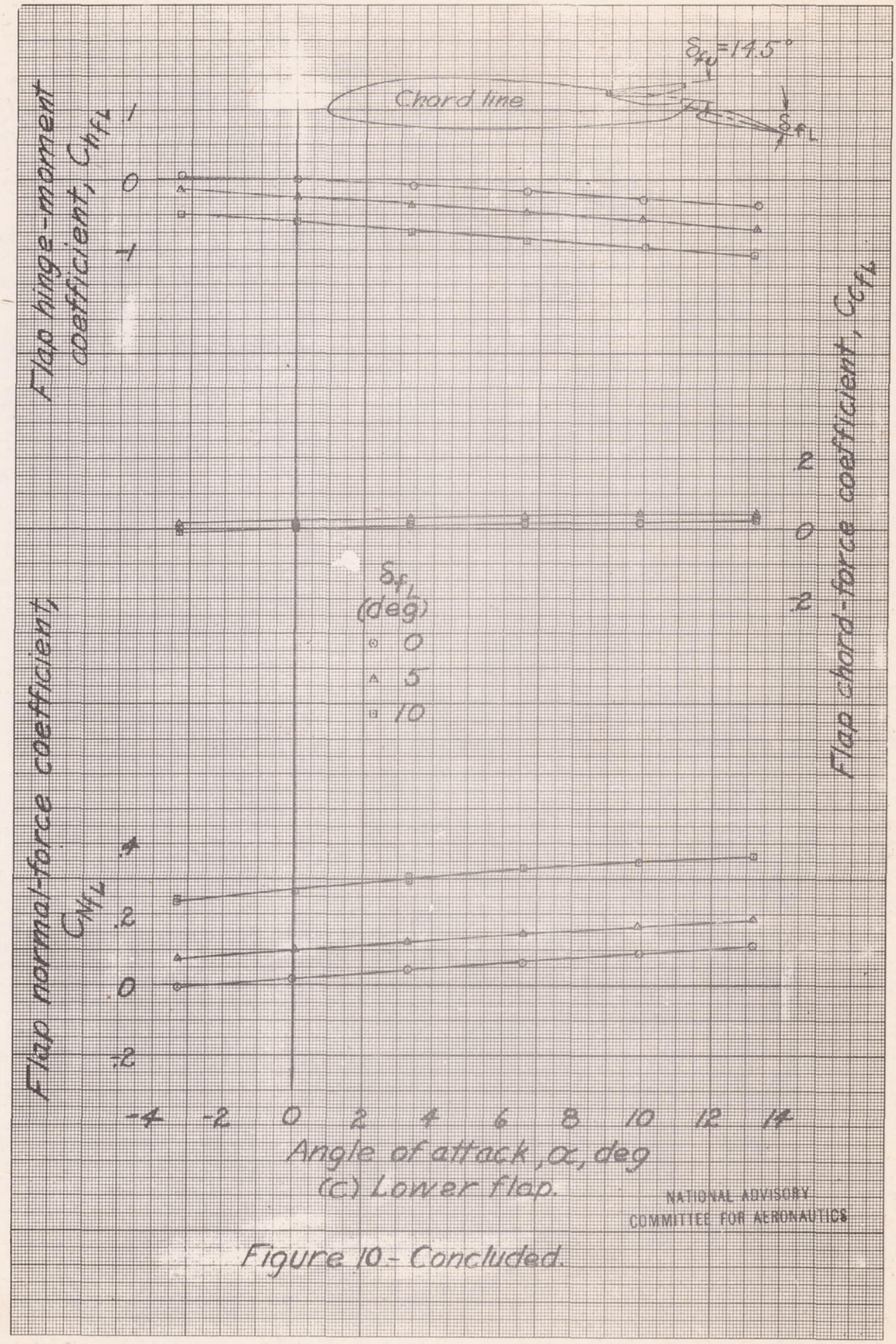

Figure 10.- Concluded.

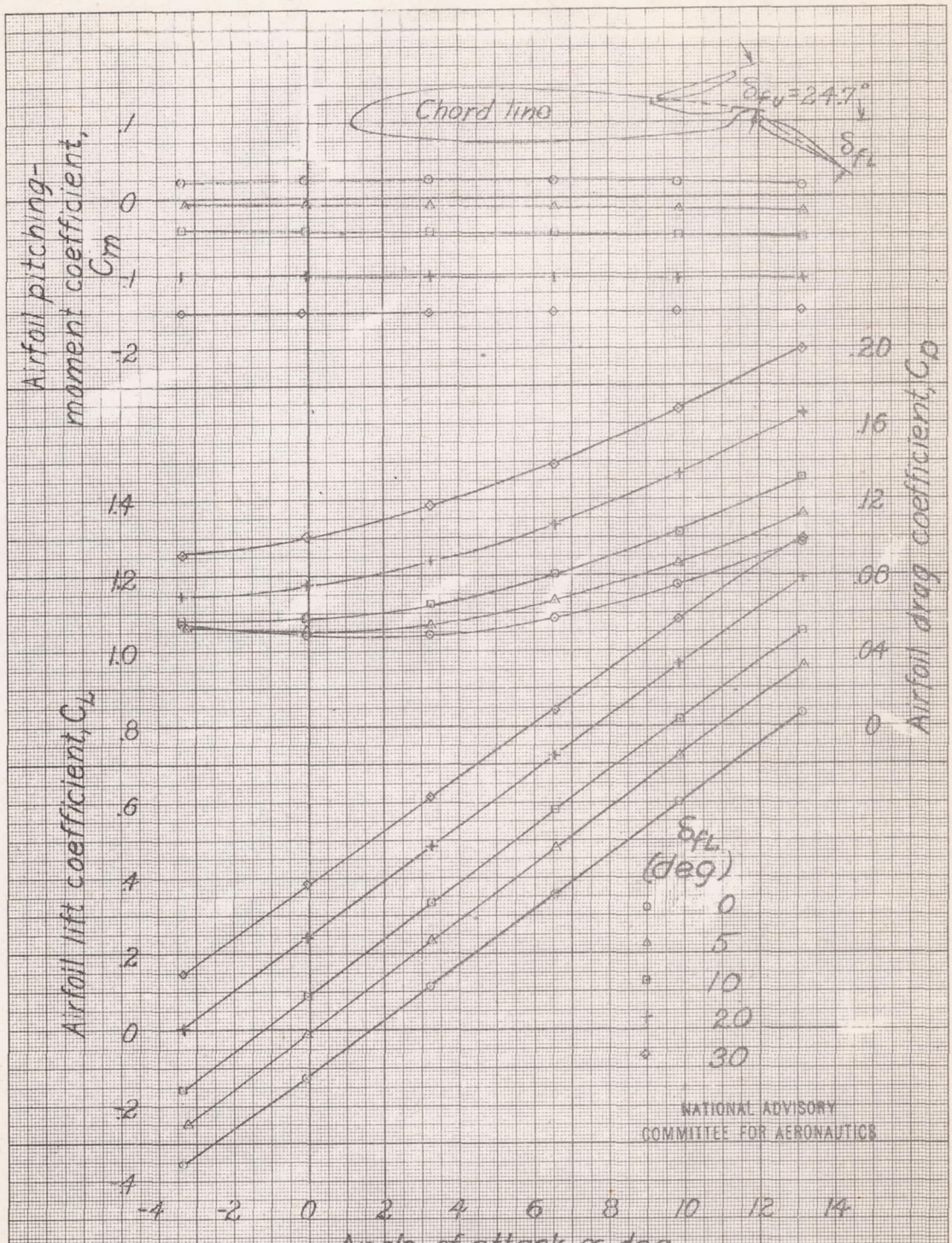

(a) Airfoil.

Figure 11.- Effect of lower flap deflection on the airfoil characteristics and flap loads of the brake-flap installation on the 0.40-scale model of the F4F-3 wing panel. δ_{fu}, 24.7°

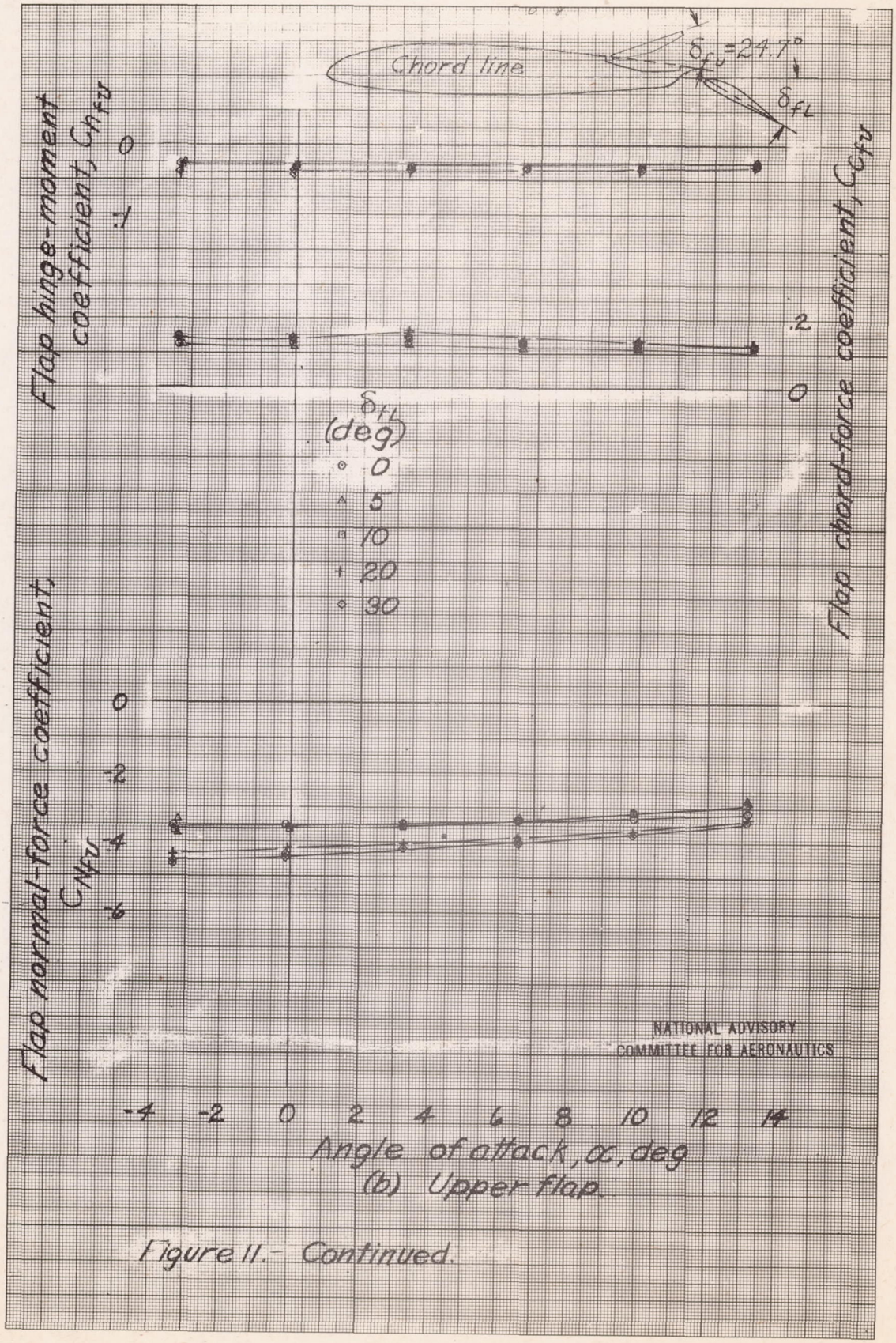

(b) Upper flap.

Figure 11.- Continued.

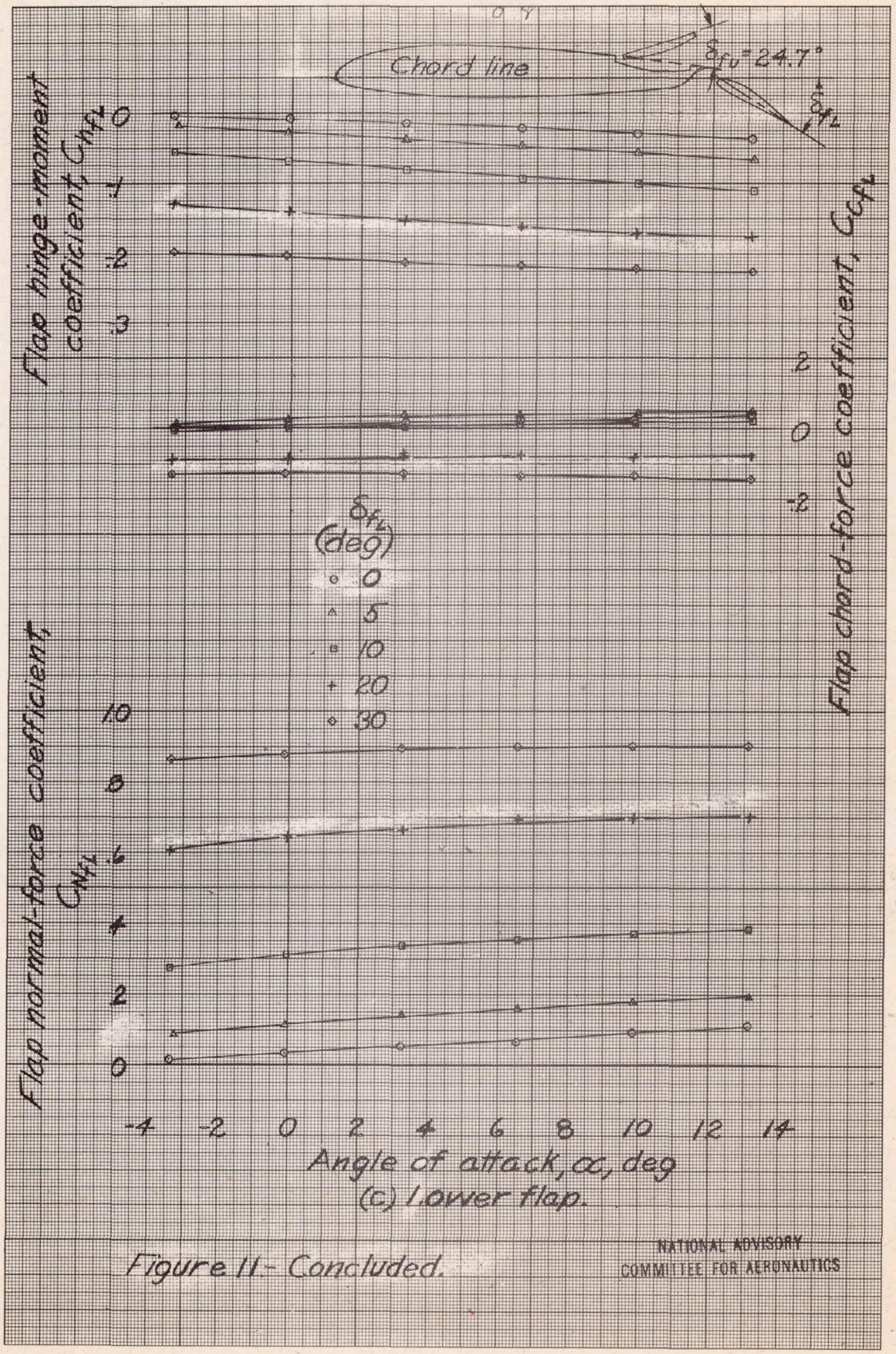

Figure 11.- Concluded.

NATIONAL ADVISORY COMMITTEE FOR AERONAUTICS

L-549

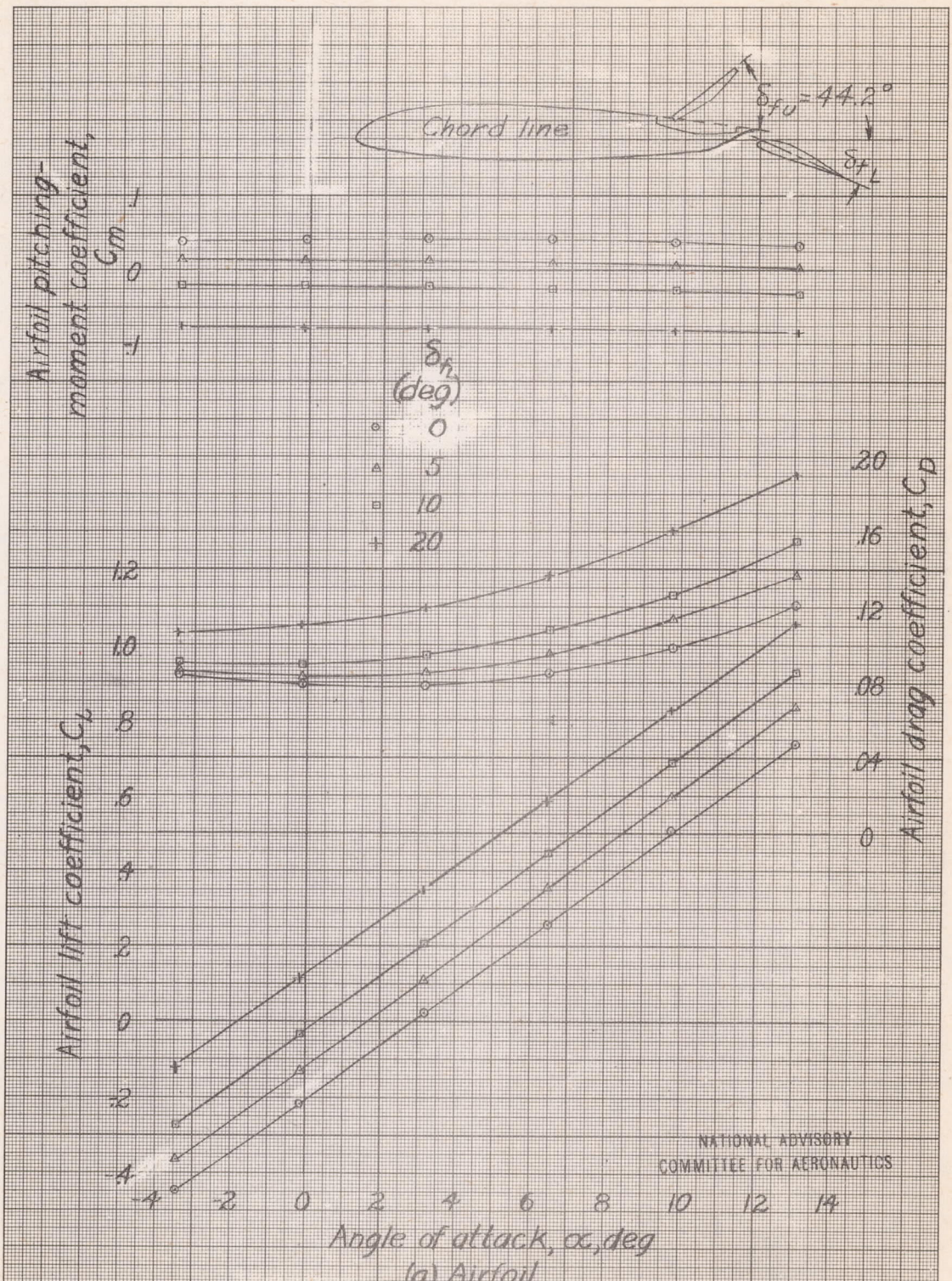

(a) Airfoil.

Figure 12 - Effect of lower flap deflection on the airfoil characteristics and flap loads of the brake-flap installation on the 0.40-scale model of the F4F-3 wing panel. δ_{fu}, 44.2°.

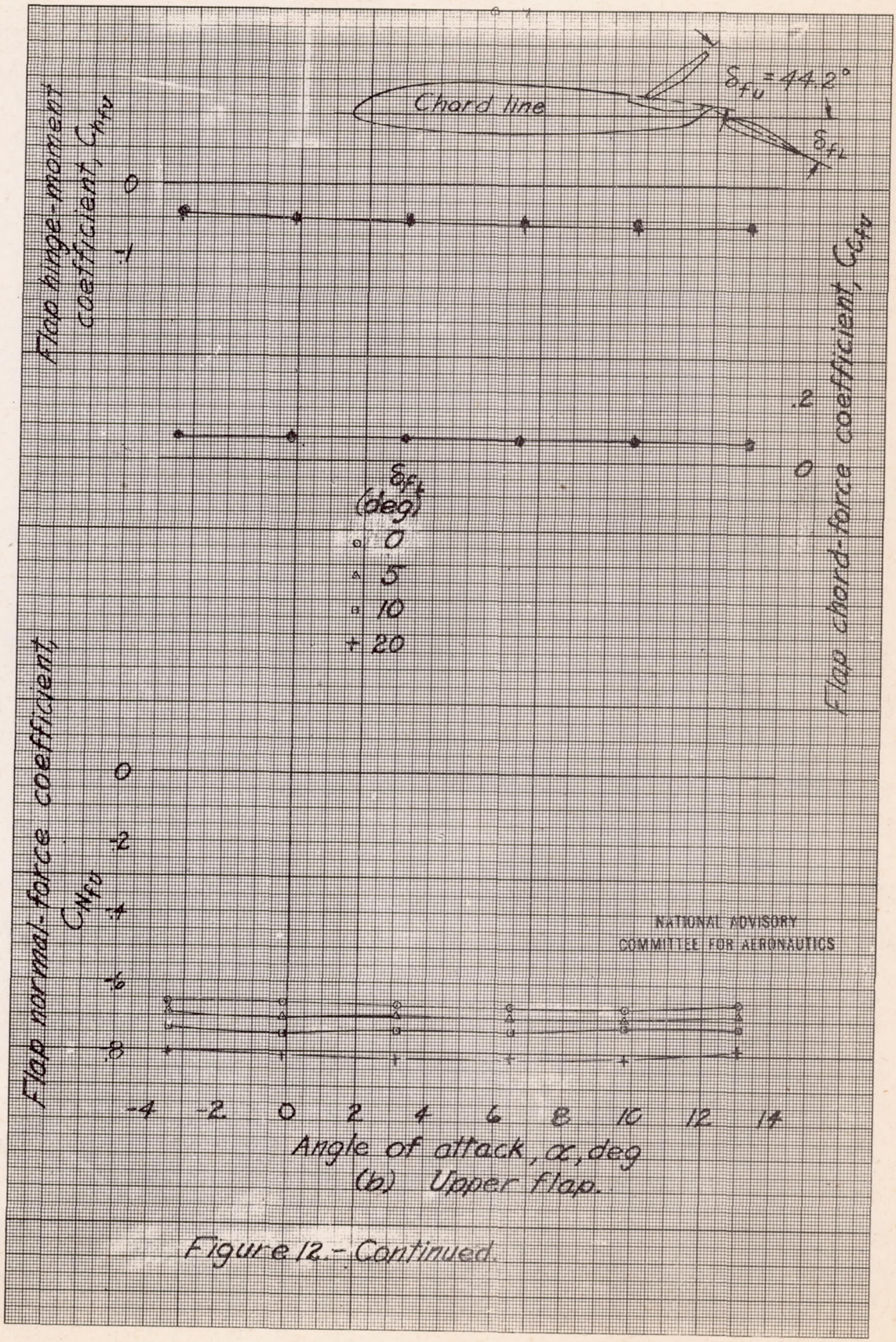

(b) Upper flap.

Figure 12.- Continued.

L-549

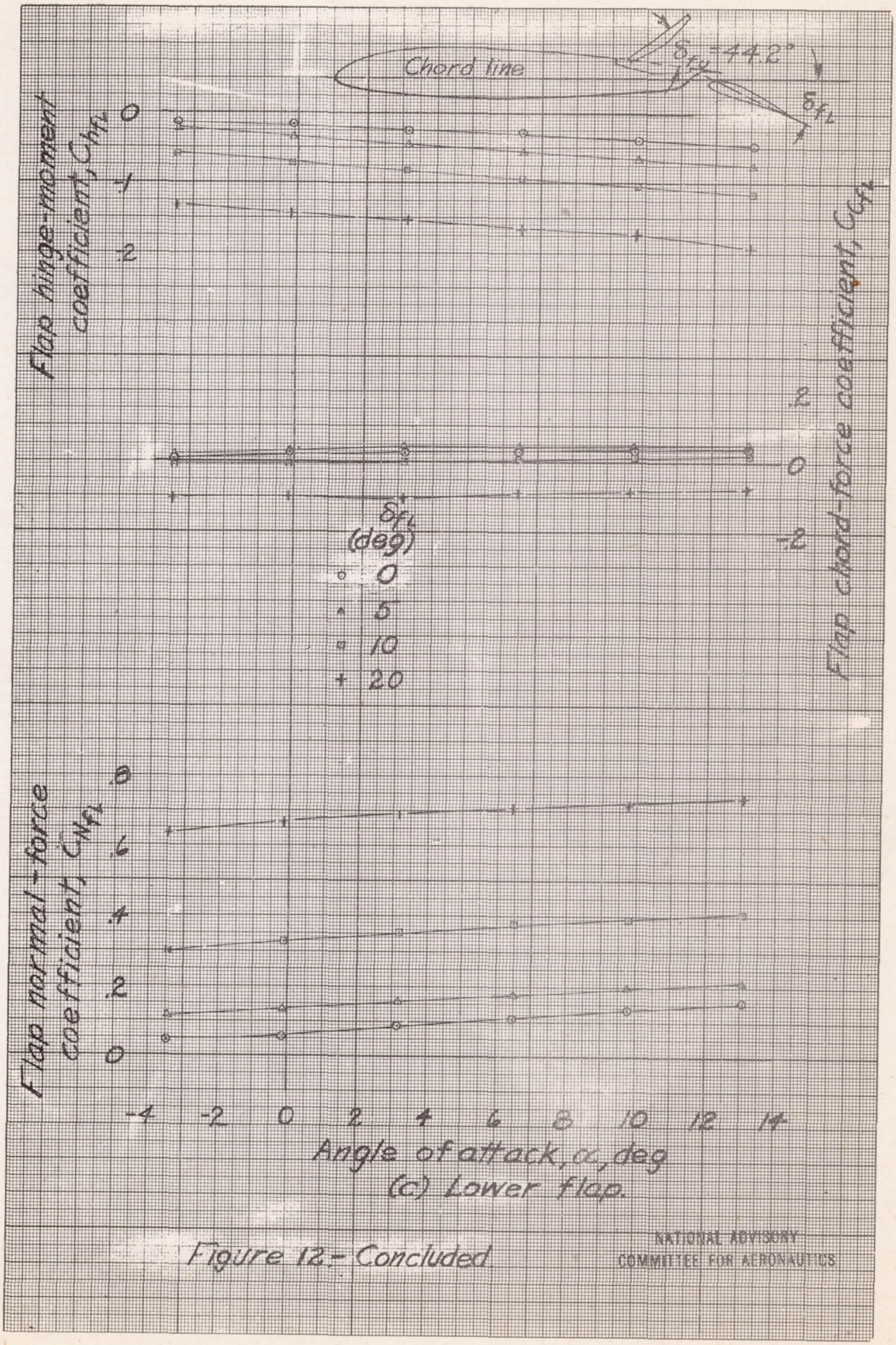

Figure 12.- Concluded

NATIONAL ADVISORY COMMITTEE FOR AERONAUTICS

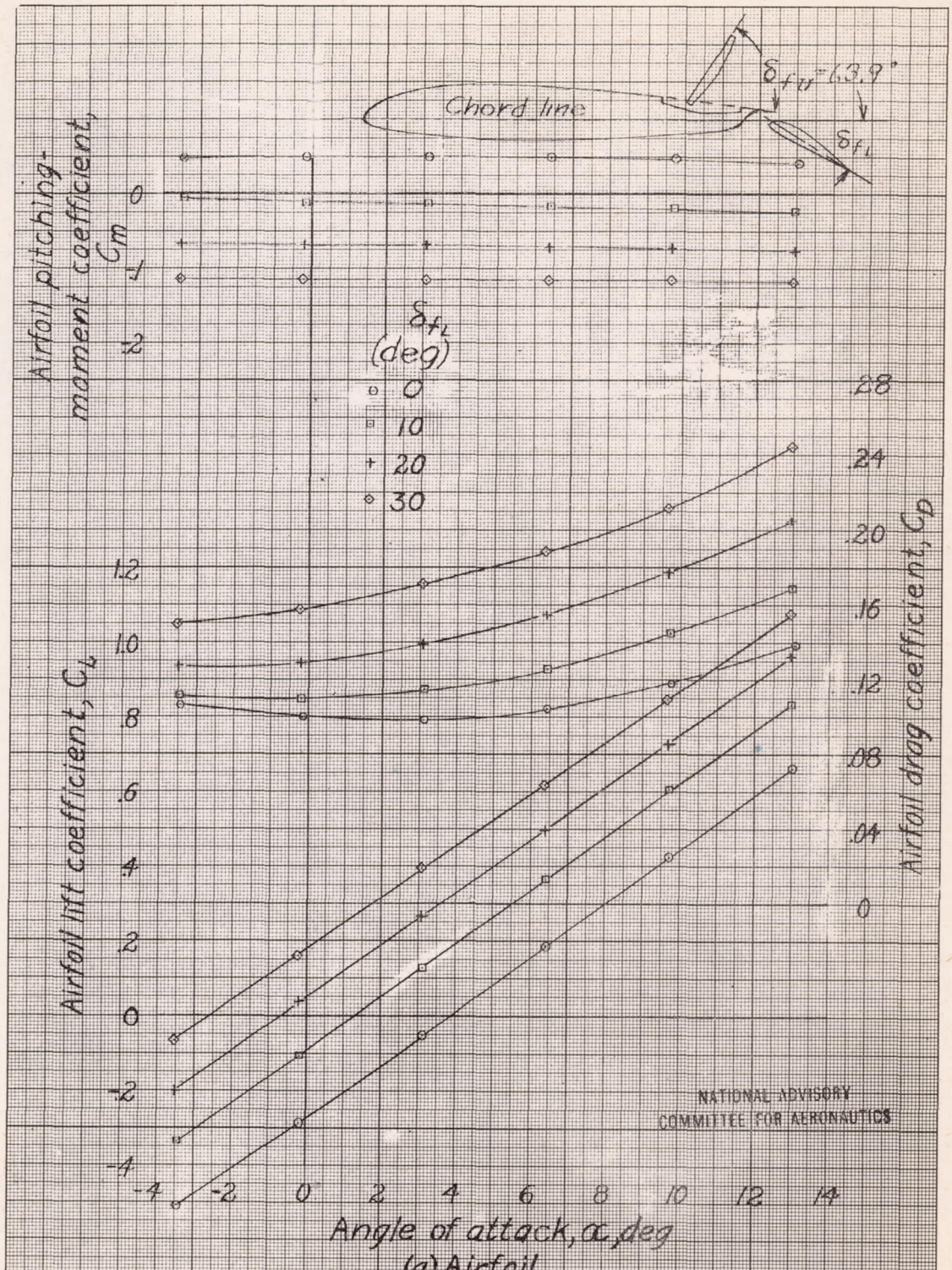

(a) Airfoil.

Figure 13.- Effect of lower flap deflection on the airfoil characteristics and flap loads of the brake-flap installation on the 0.40-scale model of the F4F-3 wing panel. δ_{f_U}, 63.9°.

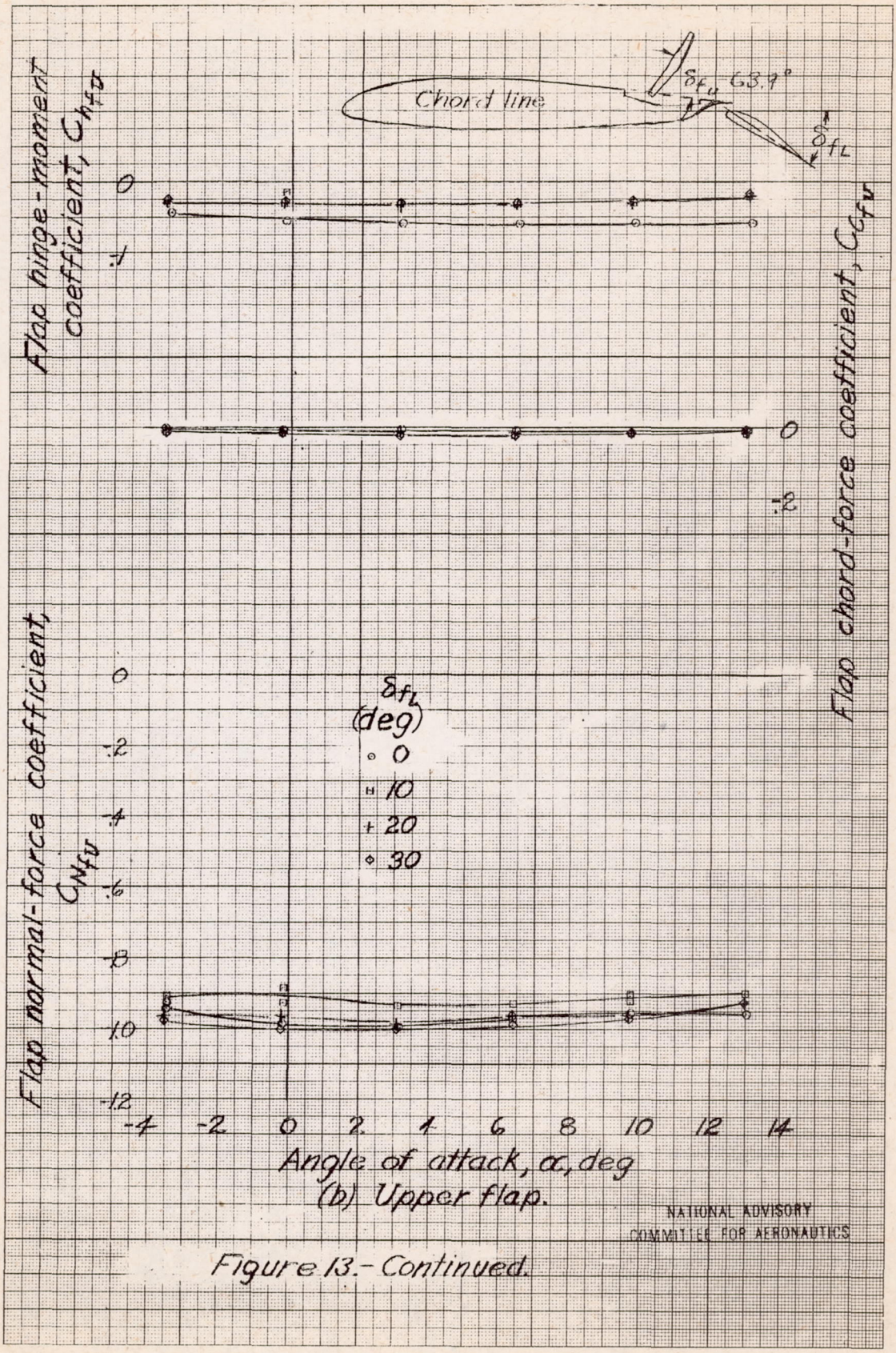

(b) Upper flap.

NATIONAL ADVISORY COMMITTEE FOR AERONAUTICS

Figure 13.- Continued.

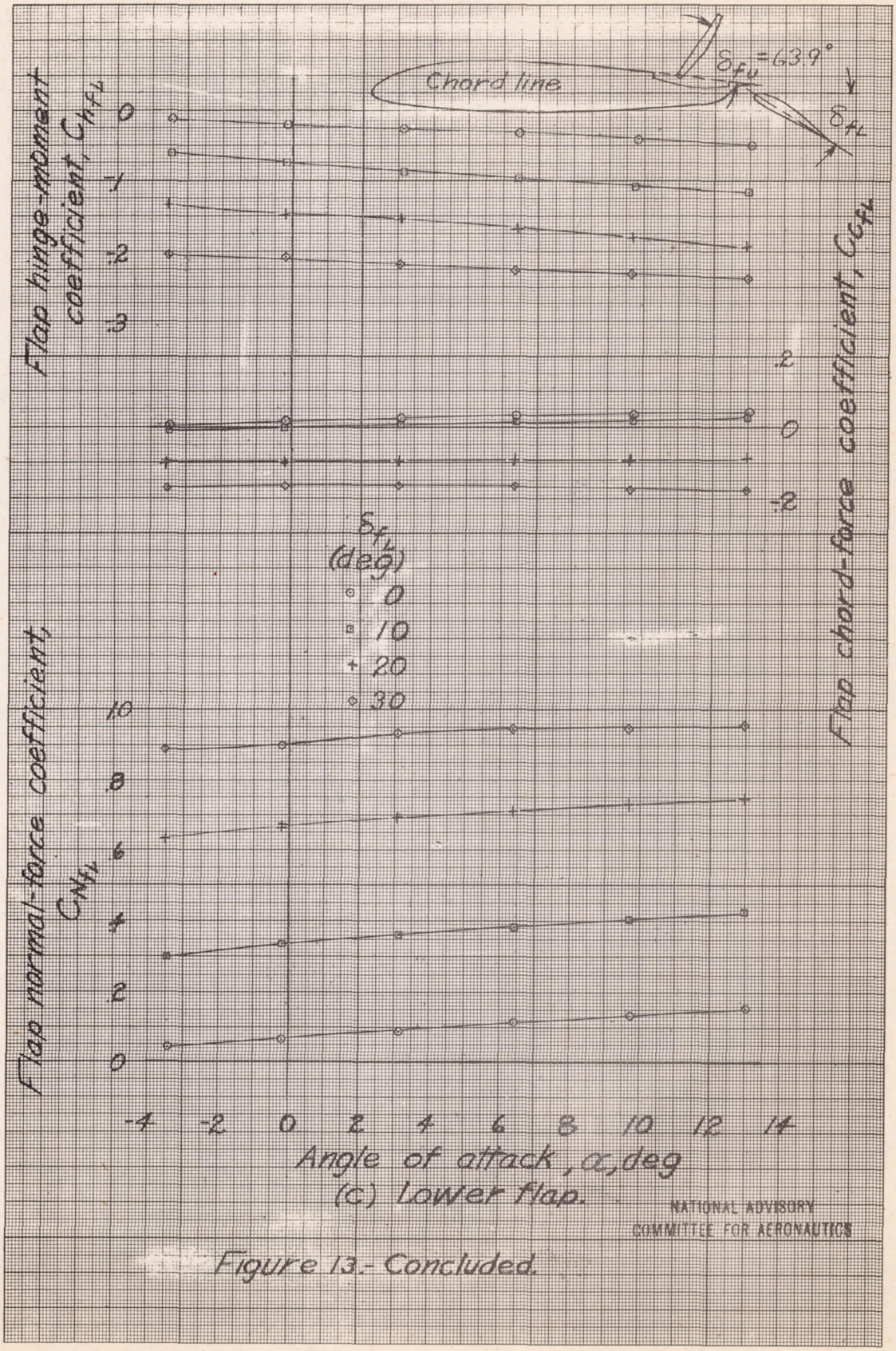

Figure 13.- Concluded.

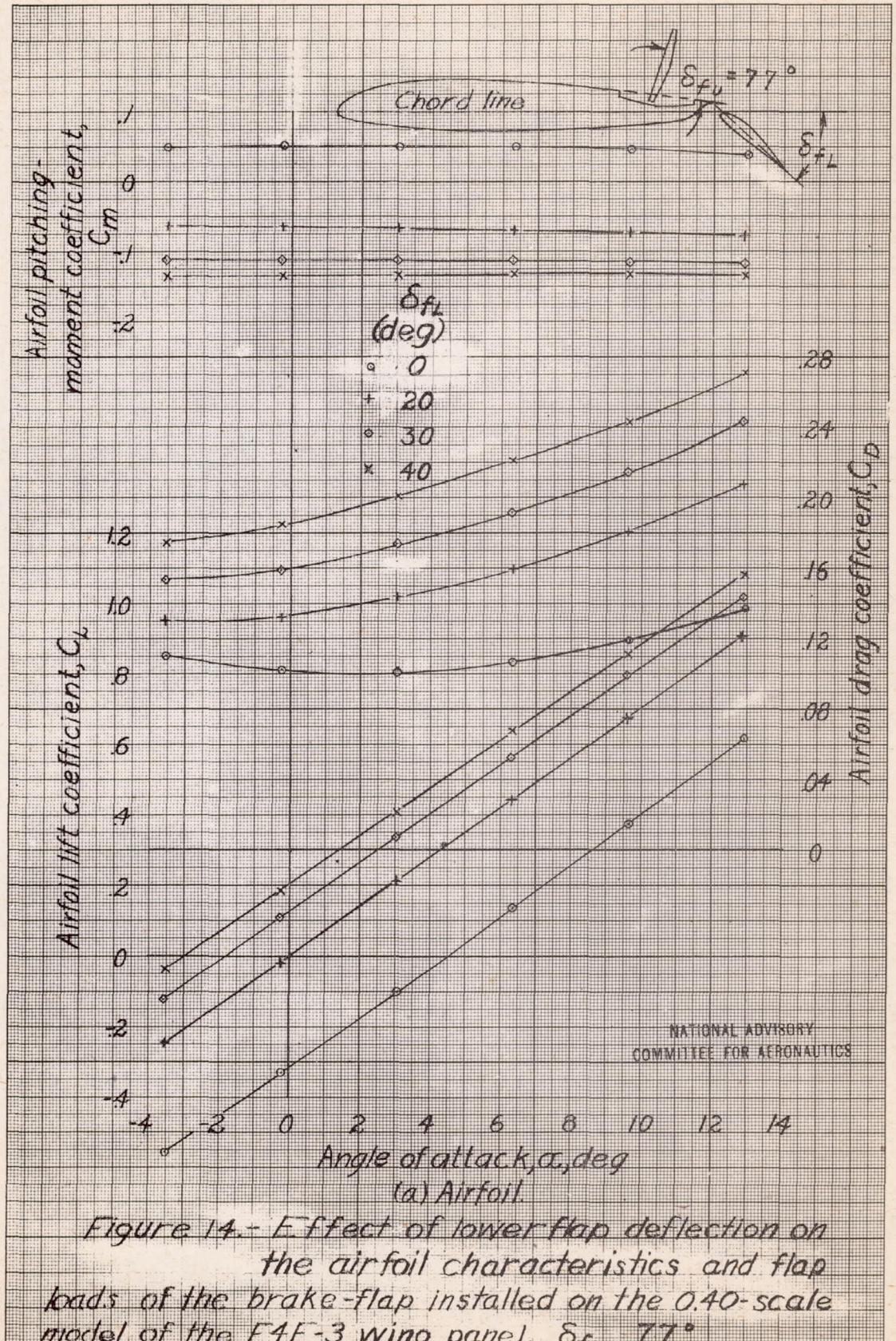

(a) Airfoil.

Figure 14.- Effect of lower flap deflection on the airfoil characteristics and flap loads of the brake-flap installed on the 0.40-scale model of the F4F-3 wing panel. δ_{fu}, 77°.

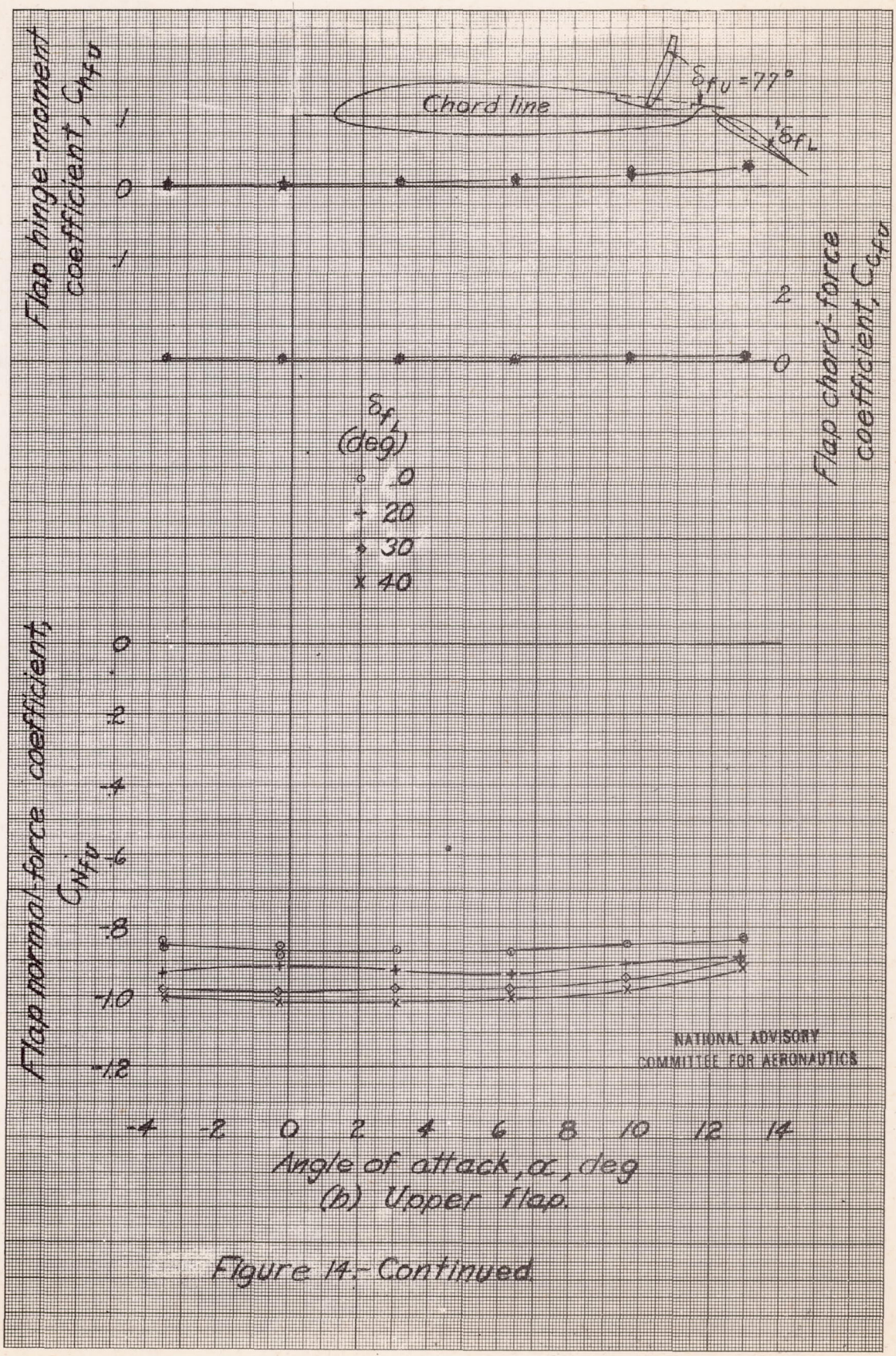

(b) Upper flap.

Figure 14.- Continued.

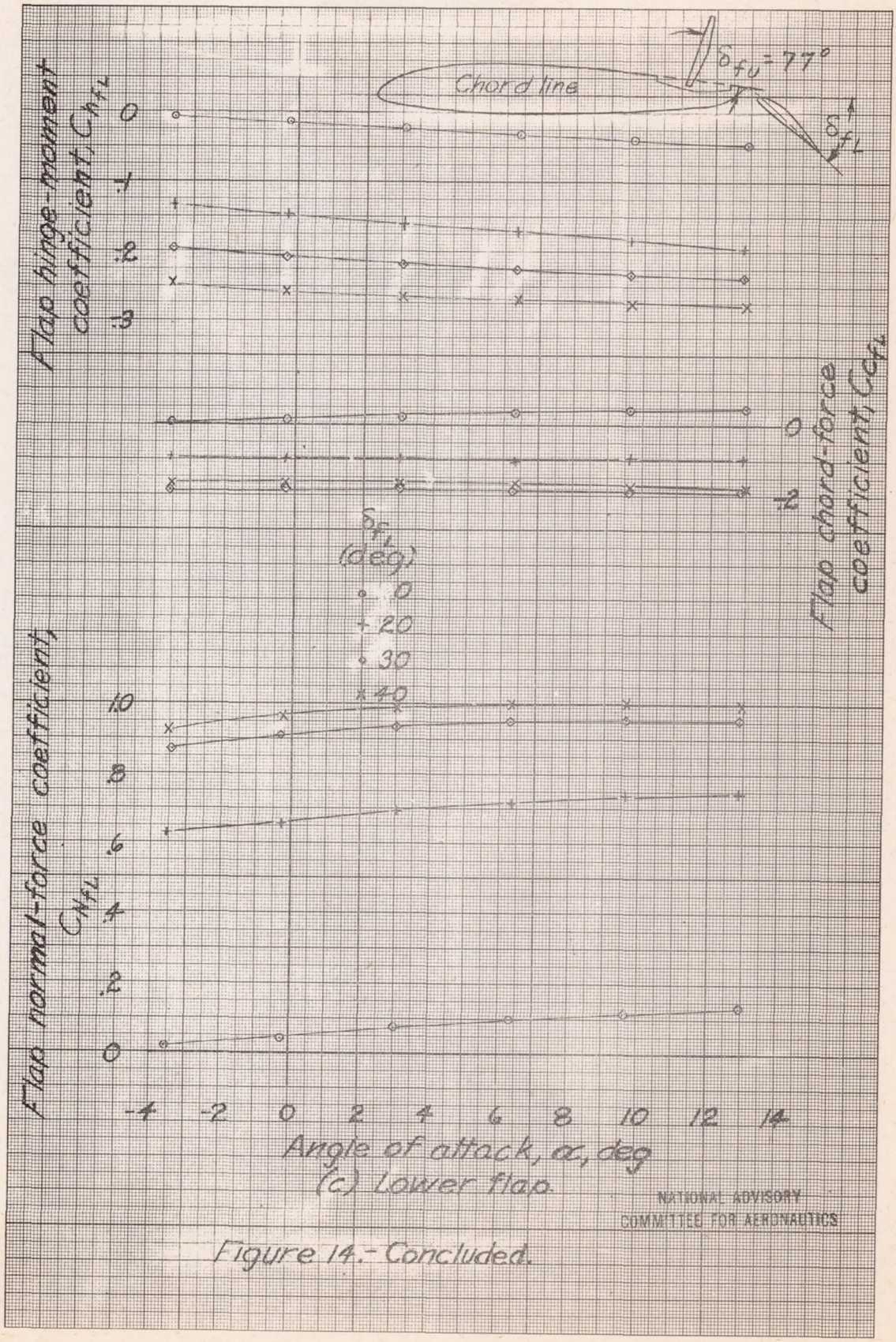

Figure 14.- Concluded.

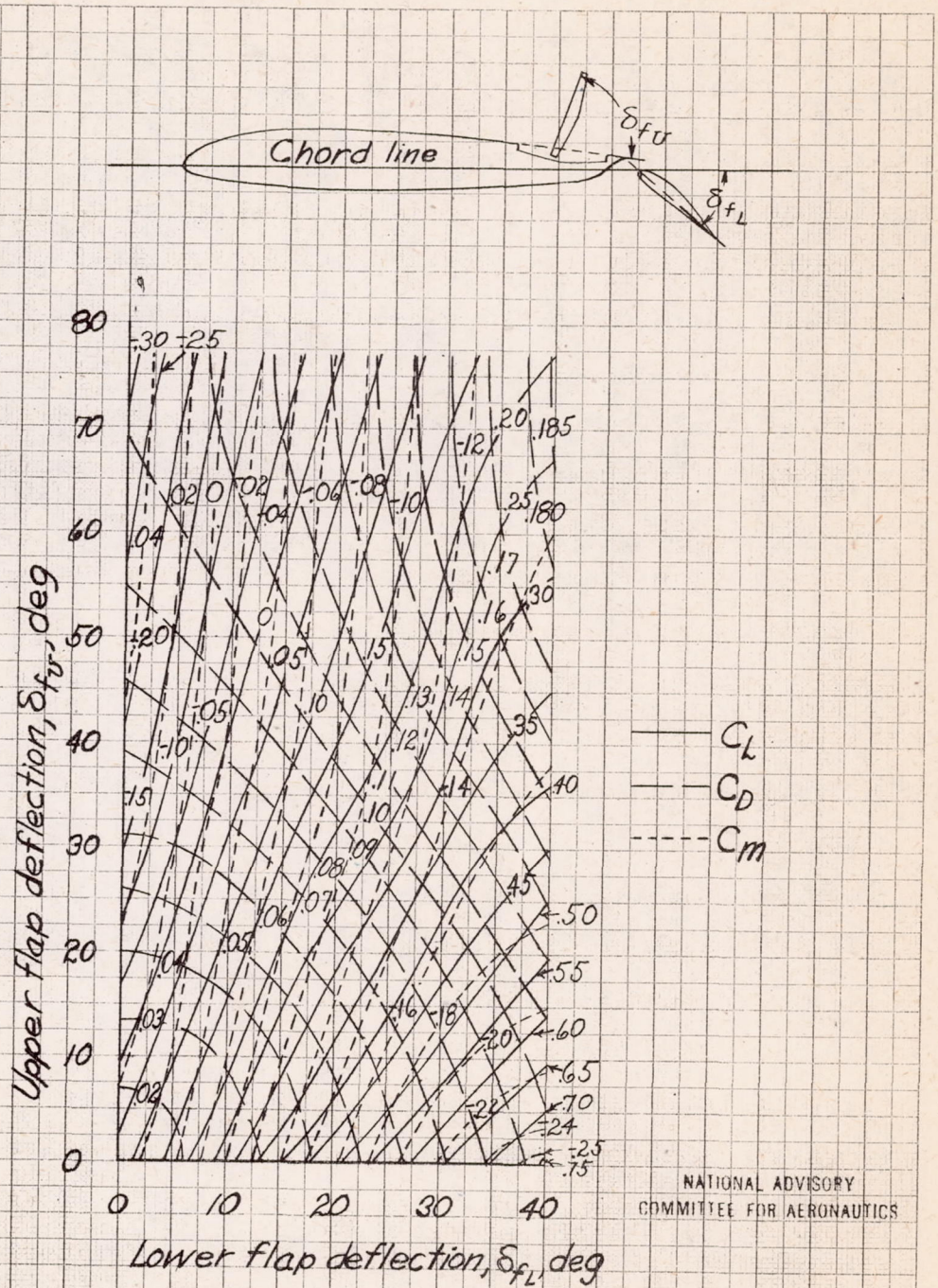

Figure 15. - Contours of C_L, C_D, and C_m at $\alpha = 0$ for the brake-flap installation on the 0.40-scale model of the F4F-3 wing panel.

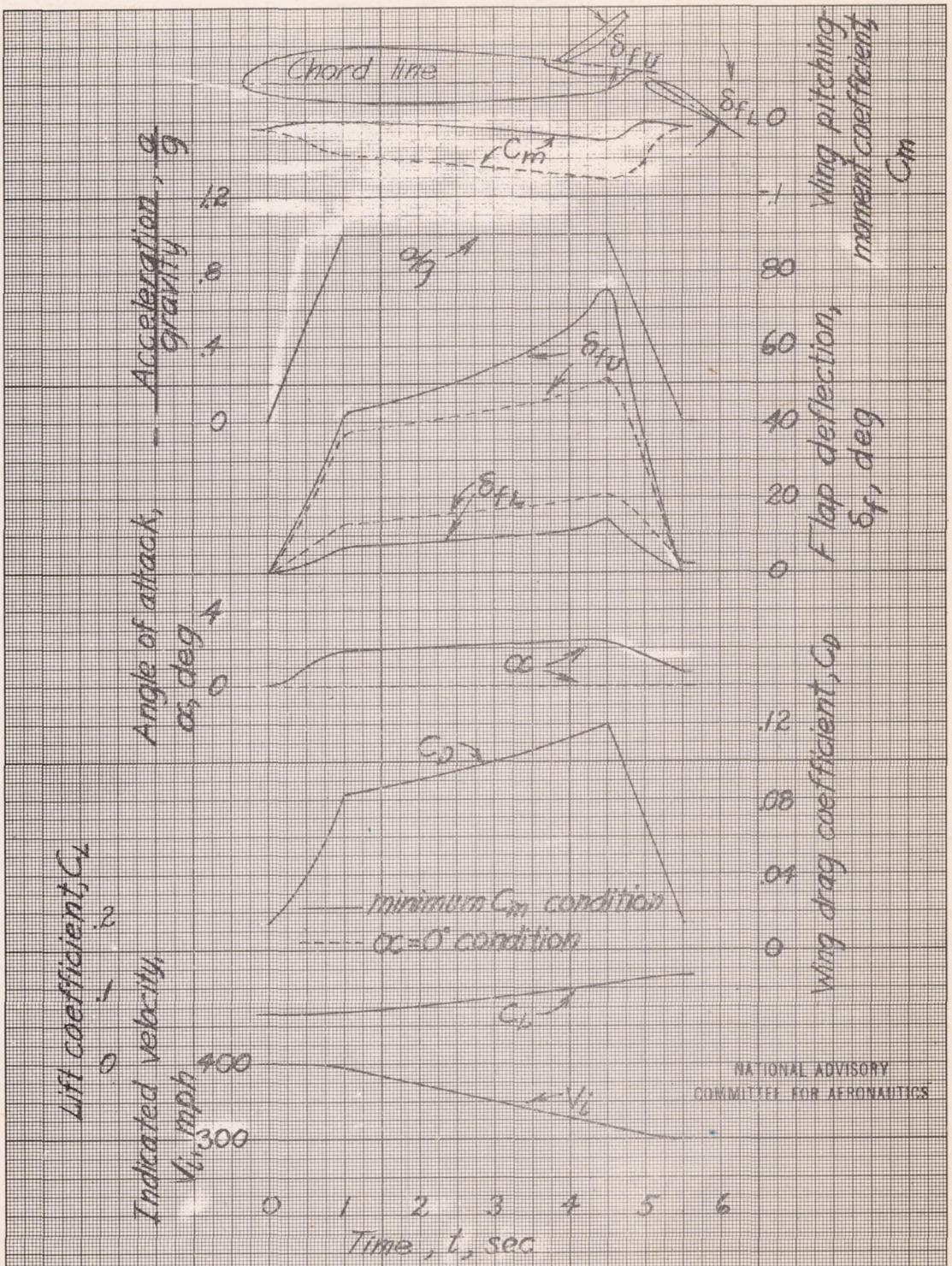

Figure 16.- Computed time-history characteristics during deceleration of the F4F-3 airplane equipped with brake flaps. Computed for sea level, a/g, 1.0(constant)

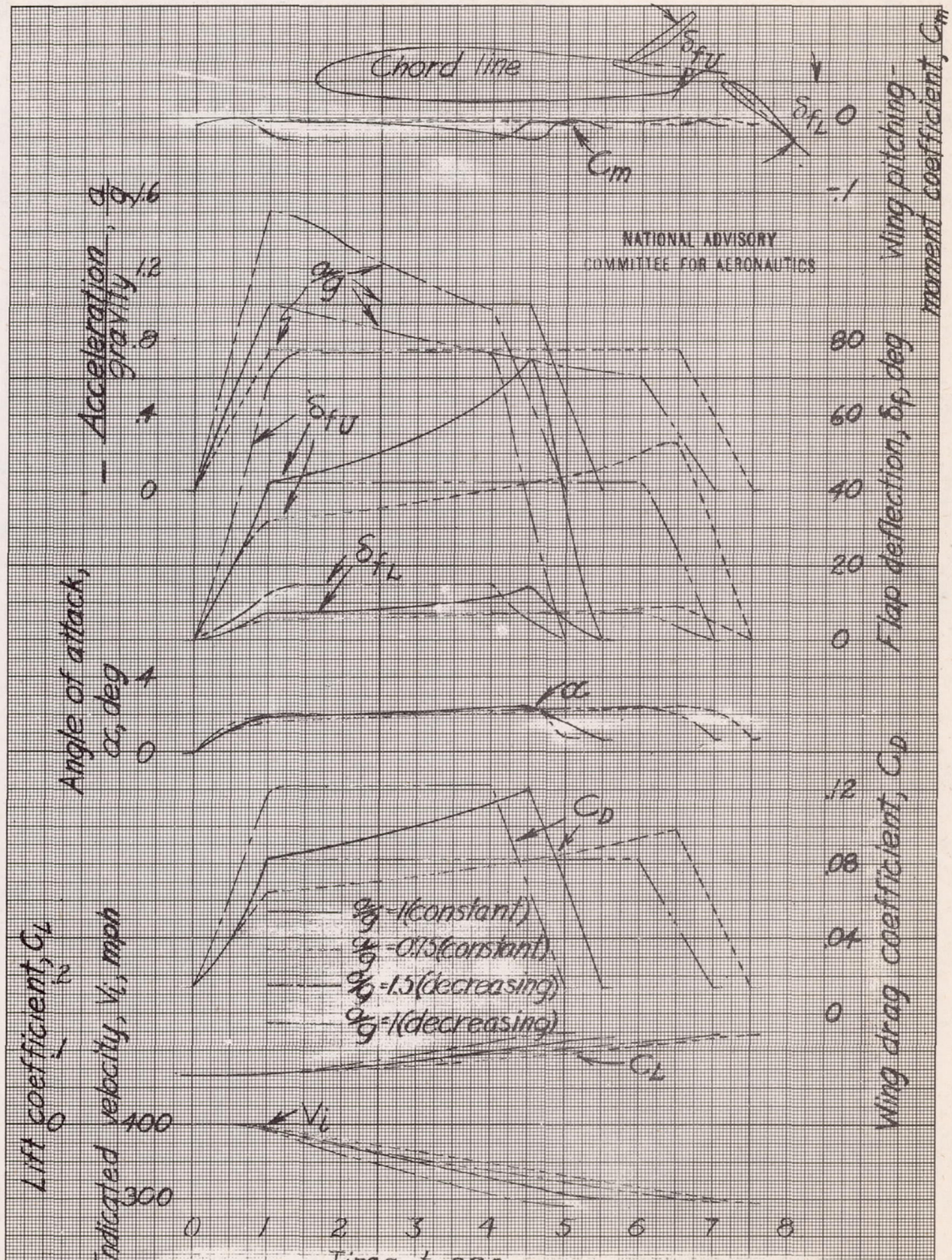

Figure 17.- Computed time-history characteristics during deceleration of the F4F-3 airplane equipped with brake flaps. Computed for sea level, minimum C_m condition.